Active Matter in two dimensions

Leticia F. Cugliandolo

Sorbonne Université

Institut Universitaire de France

leticia@lpthe.jussieu.fr
www.lpthe.jussieu.fr/˜leticia

Work in collaboration with

C. Caporusso, **G. Gonnella**, **P. Digregorio**, **G. Negro & I. Petrelli** (Bari)
L. Carenza (Bari & Istanbul)
A. Suma (Trieste, Philadelphia & Bari)
D. Levis & I. Pagonabarraga (Barcelona & Lausanne)

Cargèse, 2024




2d Active Matter

Goal

To understand the collective behavior of **bidimensional active matter**

from the **statistical physics** viewpoint

with the help of massive **numerical simulations**

and some **analytic arguments**

Active Brownian Matter

Questions – à la Statistical Physics – on bidimensional systems

- Activity (Pe) - packing fraction (ϕ) phase diagram.

- Order of, and mechanisms for, the phase transitions.

  — Correlations, fluctuations.

  — Topological defects.

- Motility Induced Phase Separation.

  — Internal structure of dense phase.

  — Mechanisms for growth of dense phase.

- Influence of particle shape, *e.g.* disks *vs.* dumbbells.

2d Active Matter

Why two dimensions ?

Melting in two dimensions is not fully understood

It poses a **theoretical** challenge

It is **experimentally** ‘easier’ than in three dimensions (...)

It is computationally lighter to **simulate** $2d$ systems than $3d$ ones

Manifold realisations of $2d$ **active matter**

Active Brownian Matter

Questions – à la Statistical Physics

- Activity (Pe) - packing fraction (ϕ) phase diagram.
- Order of, and mechanisms for, the phase transitions.
  - Correlations, fluctuations.
  - Topological defects.
- Motility Induced Phase Separation.
  - Internal structure of dense phase.
  - Mechanisms for growth of dense phase.

- Influence of particle shape, *e.g.* **disks** *vs.* dumbbells.

Active Brownian Disks

(Overdamped) Langevin equations (the standard $2d$ model)

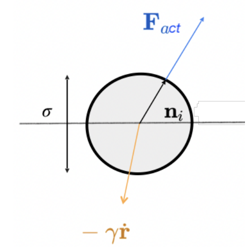

Active force $\mathbf{F}_{\rm act}$ along $\mathbf{n}_i = (\cos\theta_i, \sin\theta_i)$

$$m\ddot{\mathbf{r}}_i + \gamma\dot{\mathbf{r}}_i = F_{\rm act}\mathbf{n}_i - \nabla_i \sum_{j(\neq i)} U_{\rm Mie}(r_{ij}) + \boldsymbol{\xi}_i \;, \qquad \dot{\theta}_i = \eta_i \;,$$

$\mathbf{r}_i$ position of ith particle & $r_{ij} = |\mathbf{r}_i - \mathbf{r}_j|$ inter-part distance,

$U_{\rm Mie}$ short-range **hardly repulsive** Mie potential, over-damped limit $m/\gamma = 0.1$

$\boldsymbol{\xi}$ and η Gaussian noises with $\langle \xi_i^a(t)\rangle = \langle \eta_i(t)\rangle = 0$

$\langle \xi_i^a(t)\, \xi_j^b(t')\rangle = 2\gamma k_B T \delta_{ij}^{ab}\delta(t-t')$ with $k_BT = 0.05$, and $\langle \eta_i(t)\, \eta_j(t')\rangle = 2D_\theta\delta_{ij}\delta(t-t')$

Persistence time $\tau_p = D_\theta^{-1} = \gamma\sigma^2/(3k_BT)$. Units of length σ and energy ε.

Péclet number Pe = $F_{\rm act}\sigma/(k_BT)$ measures the activity and

$\phi = \pi\sigma^2 N/(4S)$ the packing friction

Active Brownian disks

The typical motion of particles in interaction

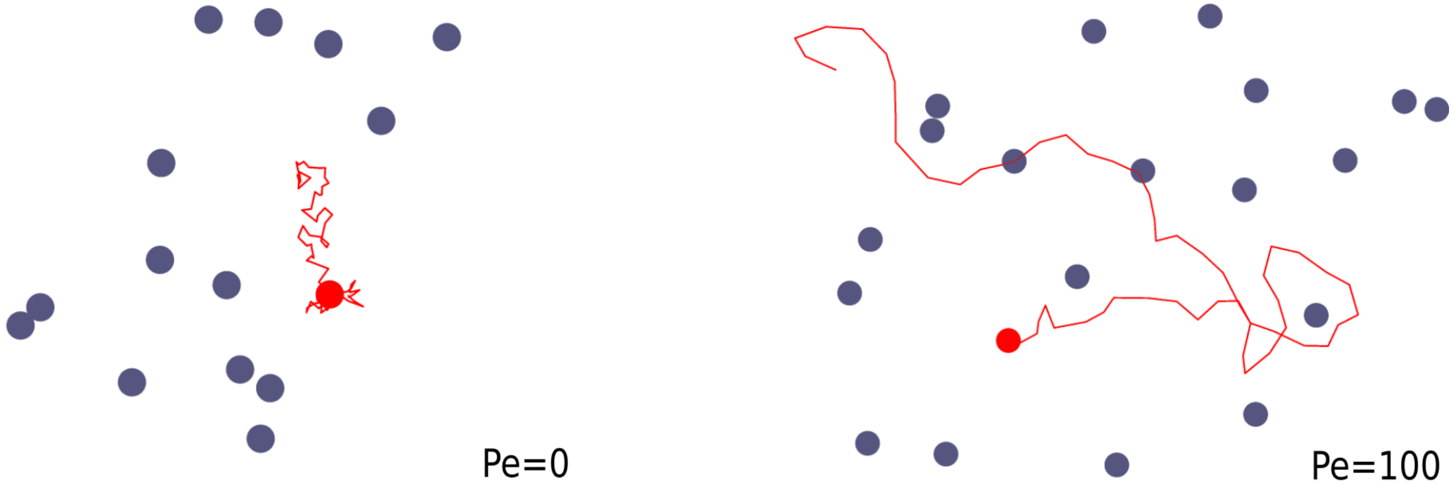

The active force induces a persistent random motion due to

$$\langle \mathbf{F}_{\rm act}(t) \cdot \mathbf{F}_{\rm act}(t') \rangle \propto F_{\rm act}^2 \, e^{-(t-t')/\tau_p}$$

with $\tau_p = D_\theta^{-1} = {}^{\gamma\sigma^2}\!/_{3k_BT}$

Active Brownian disks

Questions – à la Statistical Physics

- Pe - ϕ Phase diagram – start from solid and dilute progressively.
- Order of, and mechanisms for, the phase transitions.
  - Correlations, fluctuations.
  - Topological defects.
- Motility Induced Phase Separation.
  - Internal structure of dense phase.
  - Mechanisms for growth of dense phase.
- Influence of particle shape, *e.g.* disks *vs.* dumbbells.

Passive systems

the good old melting problem

Freezing/Melting

Two step route in passive Pe = 0 $2d$ systems

$T = 0$ Position & orientation order lost

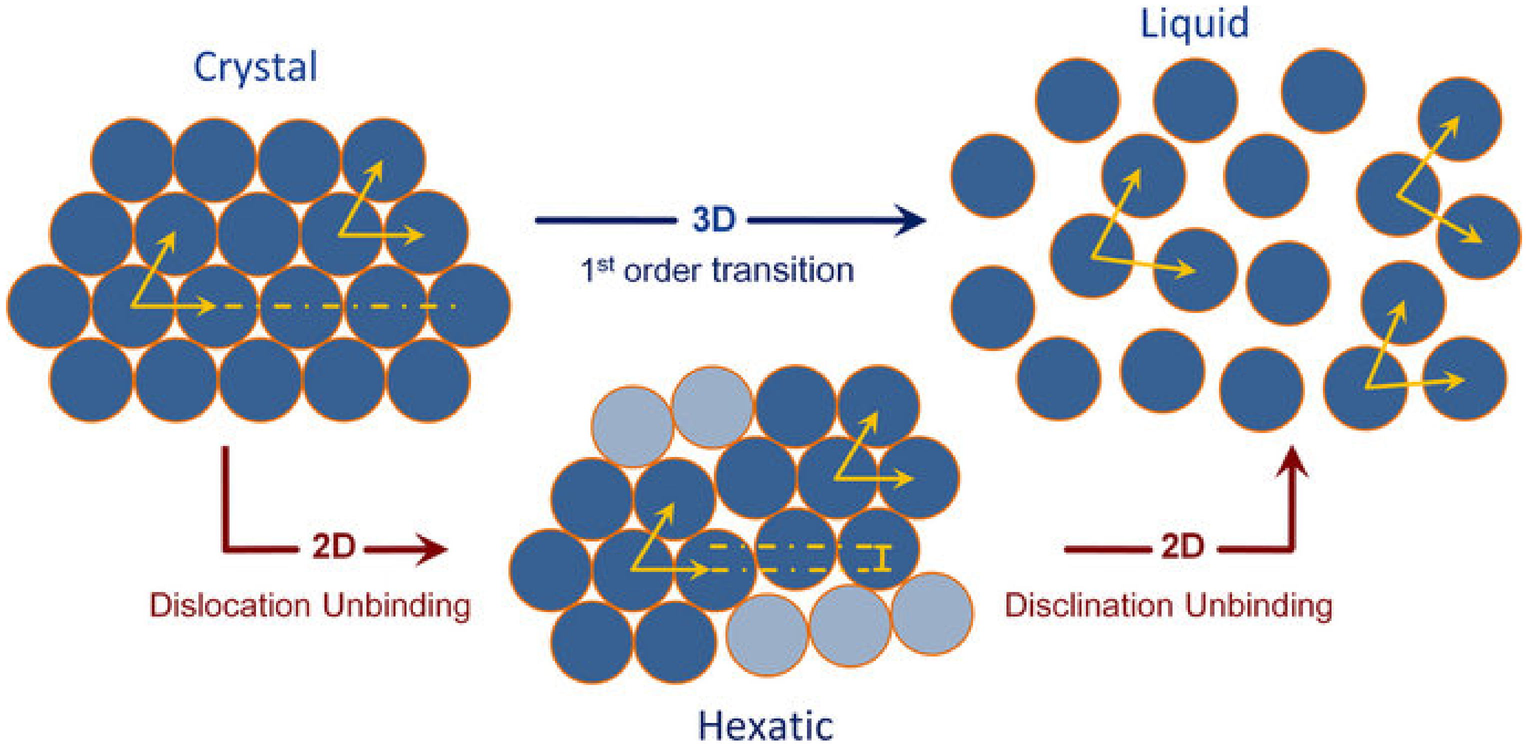

Orientation order preserved also lost

Image from **Pal, Kamal & Raghunathan, Sc. Rep. 6, 32313 (2016)**

Phases & transitions

$2d$ passive Pe = 0 systems : BKT-HNY scenario

	BKT-HNY	
Solid	QLR pos & LR orient	
transition	BKT	
Hexatic	SR pos & QLR orient	
transition	BKT	
Liquid	SR pos & orient	

Standard scenario : two step melting with two 'infinite order' transitions driven by the unbinding of defects

BKT-HNY Berezinskii-Kosterlitz-Thouless Halperin-Nelson-Young 70s

Freezing/Melting - arrows

Hexatic (orientational) order parameter $\psi_{6j} = \frac{1}{nn_j}\sum_{k=1}^{nn_j} e^{i6\theta_{jk}}$

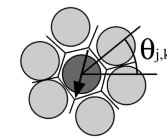

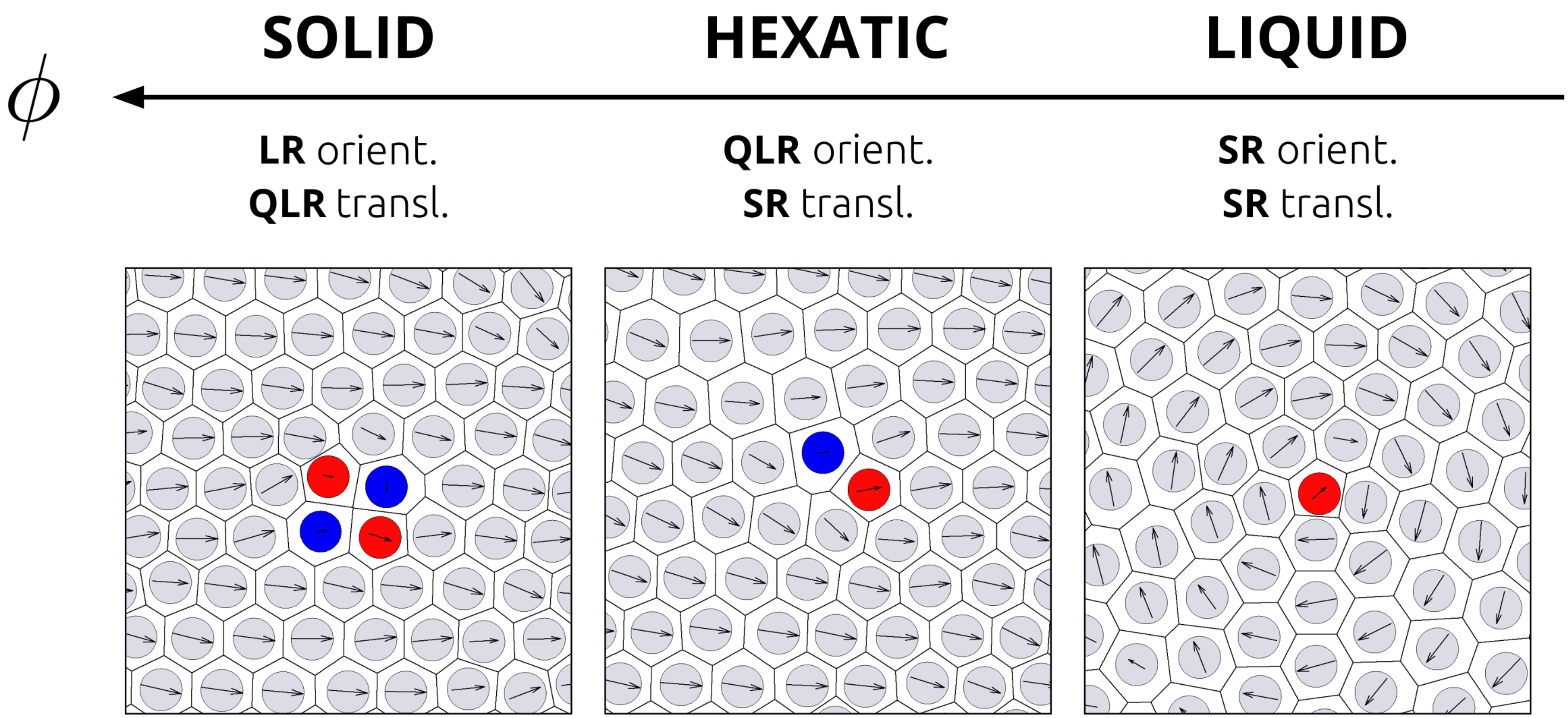

arrows oriented (LR) less oriented (QLR) order lost (SRL)

- five neighbours
- seven neighbours

Voronoi tessellation

Correlations

Hexatic orientational **Positional density-density**

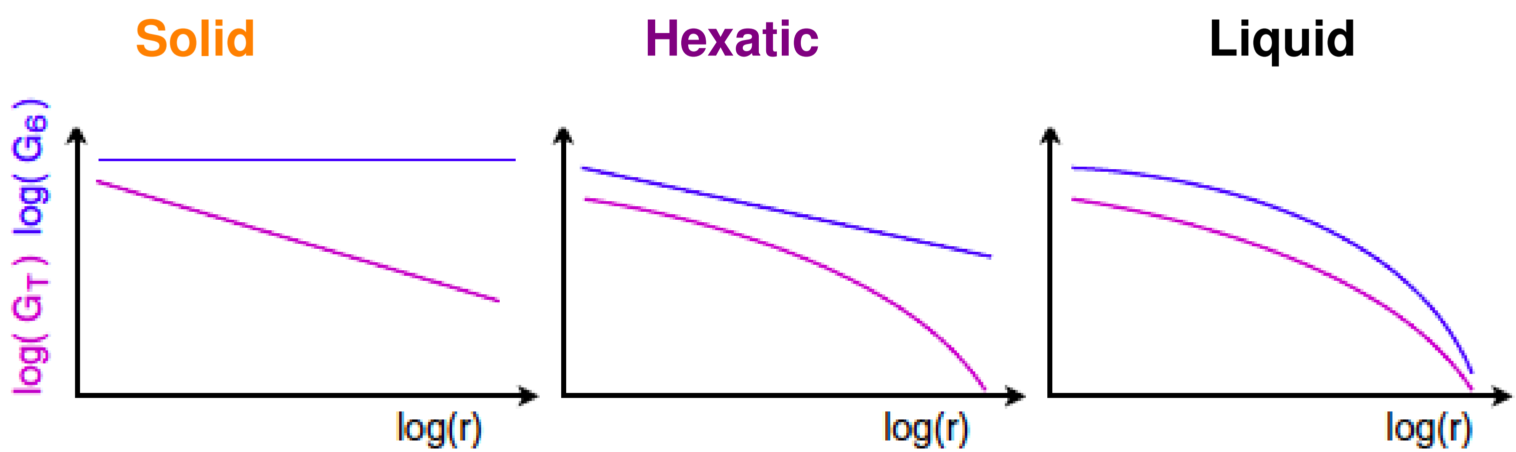

Orientational	Positional	Phase	Kind of order
G_6	G_T		
ct	$r^{-\eta}$	**Solid**	long quasi-long range order
$r^{-\eta_6}$	$e^{-r/\xi}$	**Hexatic**	quasi-long short range order
e^{-r/ξ_6}	$e^{-r/\xi}$	**Liquid**	short short range

Phases & transitions

$2d$ passive Pe = 0 systems: BKT-HNY *vs.* a new scenario

	BKT-HNY	BK
Solid	QLR pos & LR orient	QLR pos & LR orient
transition	BKT	BKT
Hexatic	SR pos & QLR orient	SR pos & QLR orient
transition	BKT	**1st order**
Liquid	SR pos & orient	SR pos & orient

Basically, the phases are the same, but the **hexatic**-**liquid** transition is different, allowing for **coexistence of the two phases** for **hard enough particles**

Event driven MC simulations. **Bernard & Krauth PRL 107, 155704 (2011)**

ABPs in the passive limit

Local density & local hexatic parameter

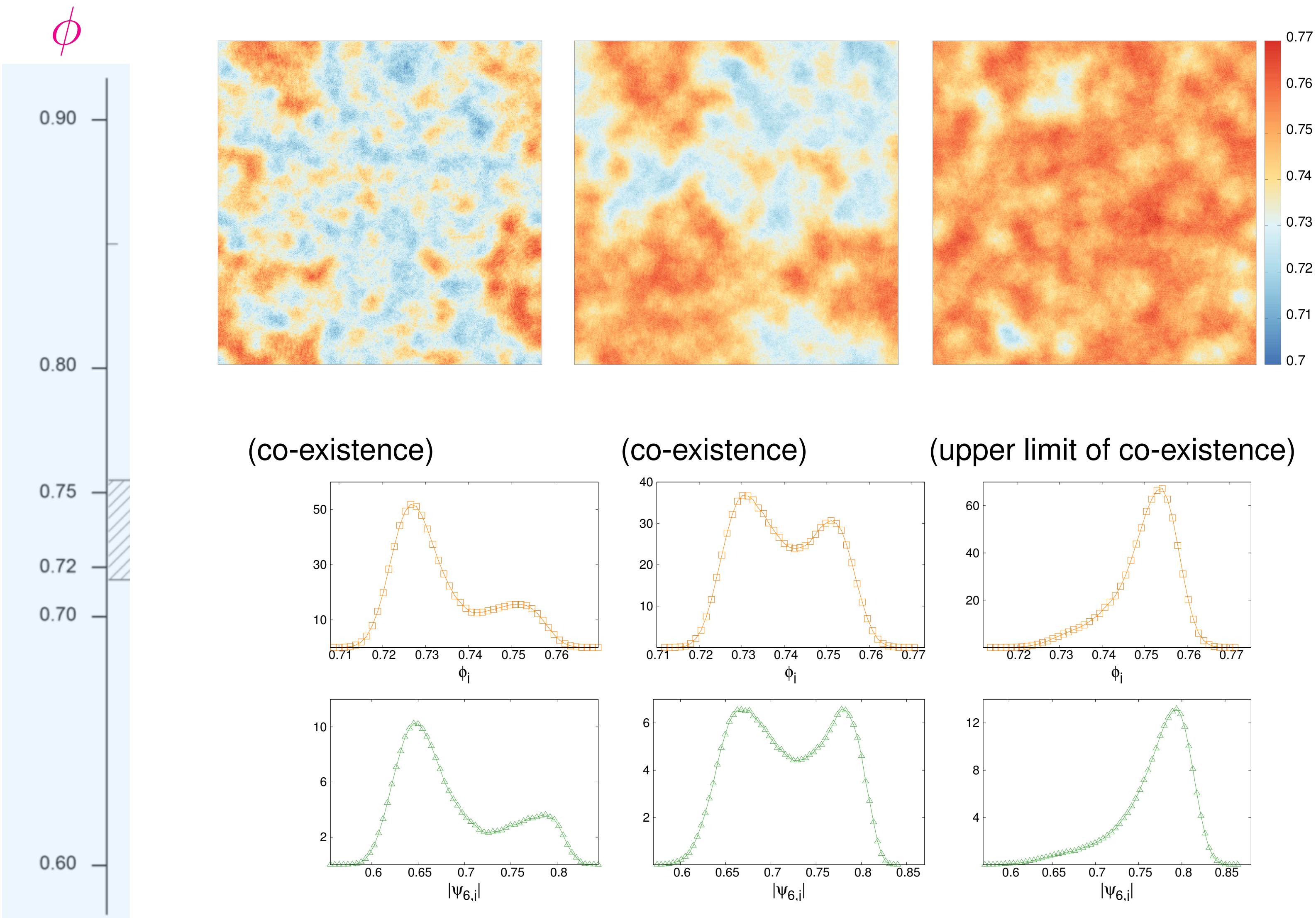

ABPs

how does the phase diagram

project into the Pe axis ?

Phase Diagram

Solid, hexatic, liquid, co-existence and MIPS

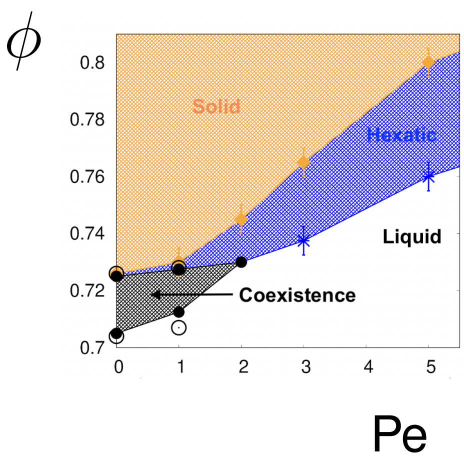

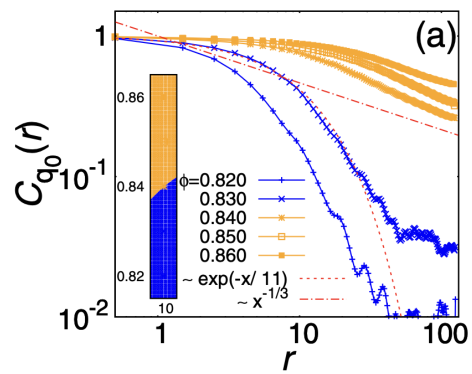

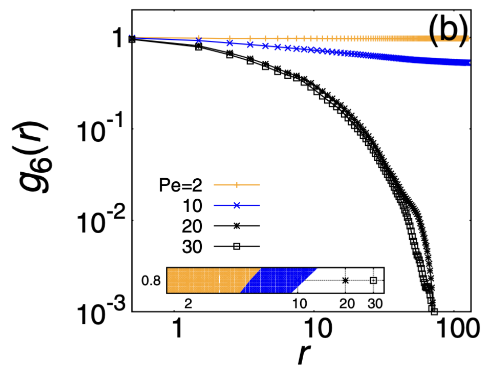

$r^{-\eta}$ $e^{-r/\xi}$ ct $r^{-\eta_6}$ e^{-r/ξ_6}

Phases characterized by

- Translational correlations $C_{q_0}(r)$ & orientational order correlations $g_6(r)$

First order **liquid** - **hexatic** transition & co-existence at low Pe from

- Pressure $P(\phi, \text{Pe})$ (Equation of State - EoS)
- Distributions of local densities ϕ_i and hexatic order parameter $|\psi_{6i}|$

Digregorio, Levis, Suma, LFC, Gonnella & Pagonabarraga, PRL 121, 098003 (2018)

Phase Diagram

Solid, hexatic, liquid, co-existence and MIPS

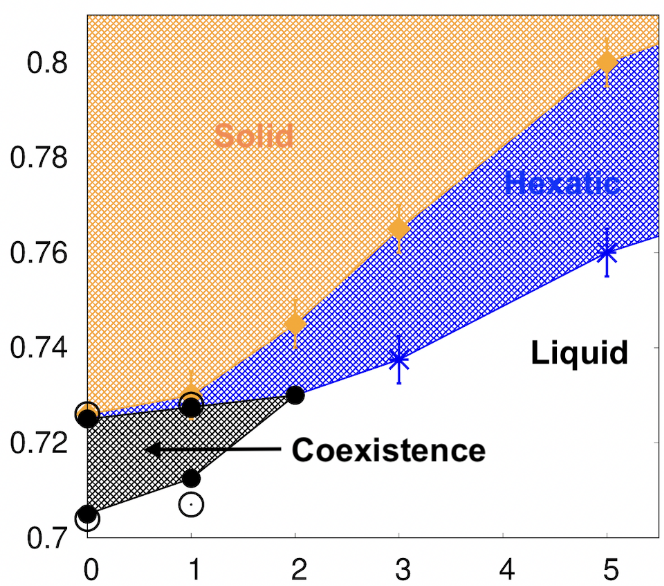

KT-HNY **solid**-**hexatic** transition

1st order **hexatic**-**liquid** close to Pe = 0

until Pe ~ 2

Different from BKTHN picture !

Pressure $P(\phi, \mathrm{Pe})$ (EOS), correlations $C_{q_0}(r)$, $g_6(r)$, and distributions of ϕ_i, $|\psi_{6i}|$

defect identification & counting

Digregorio, Levis, Suma, LFC, Gonnella & Pagonabarraga, PRL 121, 098003 (2018)

Mechanism for the transitions ?

Unbinding of point-like topological defects ?

Phases & transitions

$2d$ passive Pe = 0 systems : BKT-HNY scenario

	BKT-HNY	
Solid	QLR pos & LR orient	
transition	BKT (unbinding of dislocations)	
Hexatic phase	SR pos & QLR orient	
transition	BKT (unbinding of disclinations)	
Liquid	SR pos & orient	

Standard scenario : two step melting with two ‘infinite order’ transitions driven by the unbinding of defects

BKT-HNY Berezinskii-Kosterlitz-Thouless Halperin-Nelson-Young 70s

BKT-HNY theory

Solid-hexatic transition & the emergence of the liquid

Exponential decrease of the number density of defects at the transition

coming from the disordered side $\phi \to \phi_c^-$

$$\rho_d \sim a \;\exp\left[-b\left(\frac{\phi_c}{\phi_c-\phi}\right)^{\nu}\right]$$

Disclination $\xrightarrow{\hspace{3em}}$ 5

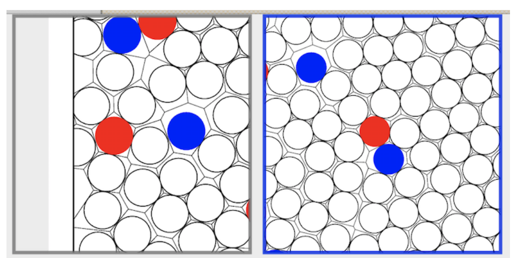

Dislocation $\xleftarrow{\hspace{3em}}$ 5 7

with $\nu = 0.37$ for dislocations at the **solid** - **hexatic** transition

and $\nu = 0.5$ for disclinations at the **hexatic** - **liquid** transition

Mechanisms

Unbinding of dislocations & disclinations ?

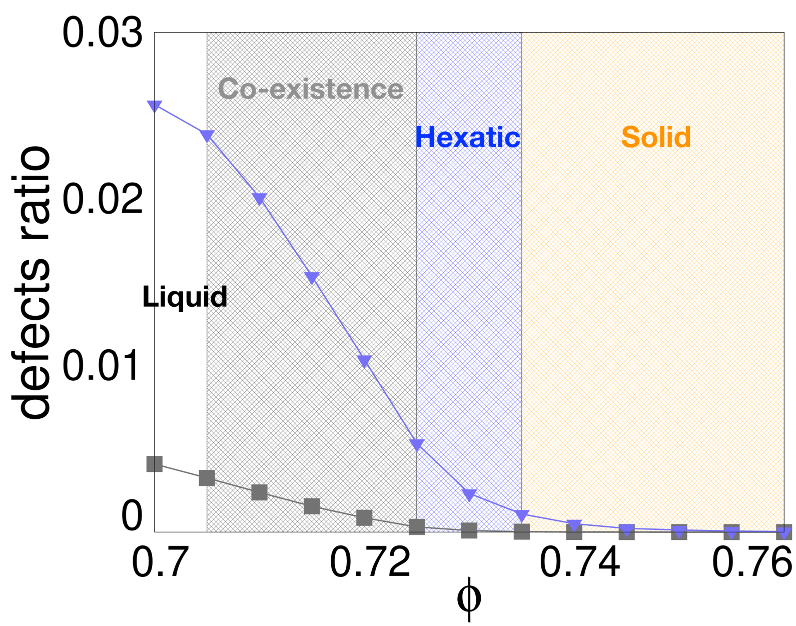

5 & 7 neighbors

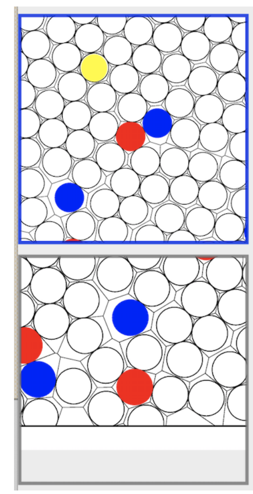

Dislocations ▼ unbind at the **solid** - **hexatic** transition as in BKT-HNY theory

$$\rho_{dislocations} \sim a \ \exp\left[-b\left(\frac{\phi_c}{\phi_c-\phi}\right)^{\nu}\right] \qquad \nu \sim 0.37 \ \forall \text{ Pe}$$

Disclinations ■ unbind when the **liquid** appears in the co-existence region

Digregorio et al. Soft Matter 18, 566 (22) ; experiments Han, Ha, Alsayed & Yodh, PRE 77, 041406 (08)

Topological defects

Summary of results

- **Solid** - **hexatic** à la BKT-HNY even quantitatively (ν value) and independently of the activity (Pe) $\boxed{\textit{Universality}}$ (with respect to ν)

- **Hexatic** - **liquid** very few disclinations and not even free

  $\boxed{\textit{Breakdown of the BKT-HNY picture for all Pe (even zero)}}$

- Close to, but in the liquid, $\boxed{\textbf{percolation}\ \text{of}\ \textit{clusters of defects}}$ with properties of uncorrelated critical percolation ($d_{\rm f}, \tau$)

- In **MIPS**, network of defects on top of the interfaces between hexatically ordered regions, interrupted by the *gas bubbles in cavitation*

Digregorio, Levis, Cugliandolo, Gonnella, Pagonabarraga, Soft Matter 18, 566 (2022)

Solid-hexatic

driven by unbinding of dislocation

For all Pe ✔

Universality ?

Hexatic-liquid

Disclinations ?

Disclinations

At the hexatic - liquid transition ϕ_l at all Pe

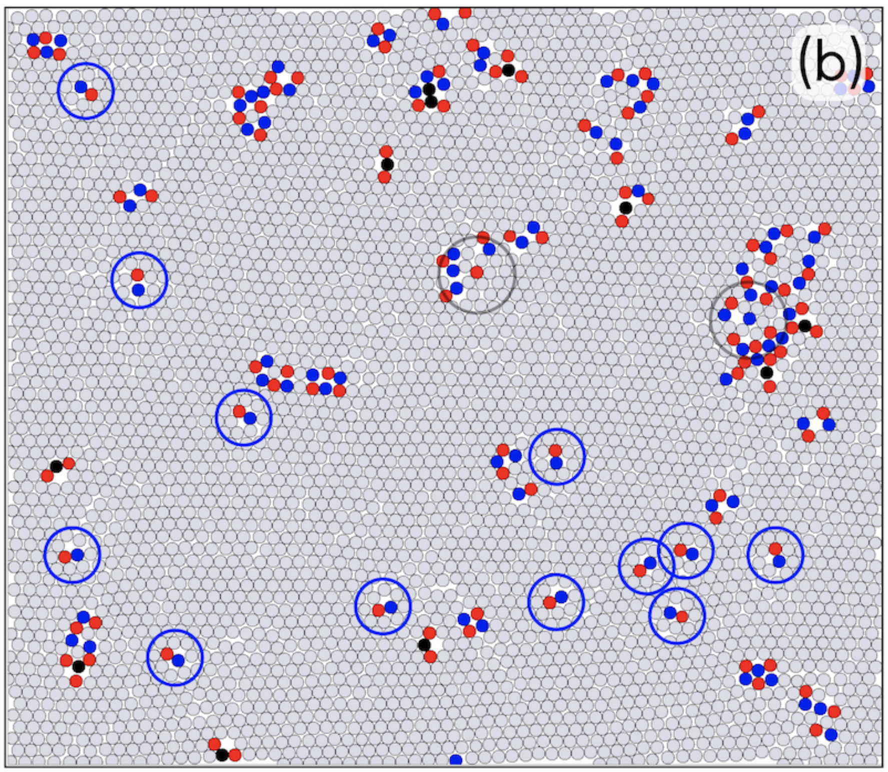

dislocations

disclinations

Very few disclinations, and always very close to other defects, so **not free**

Clusters of nn defected particles

Close to the hexatic - liquid transition

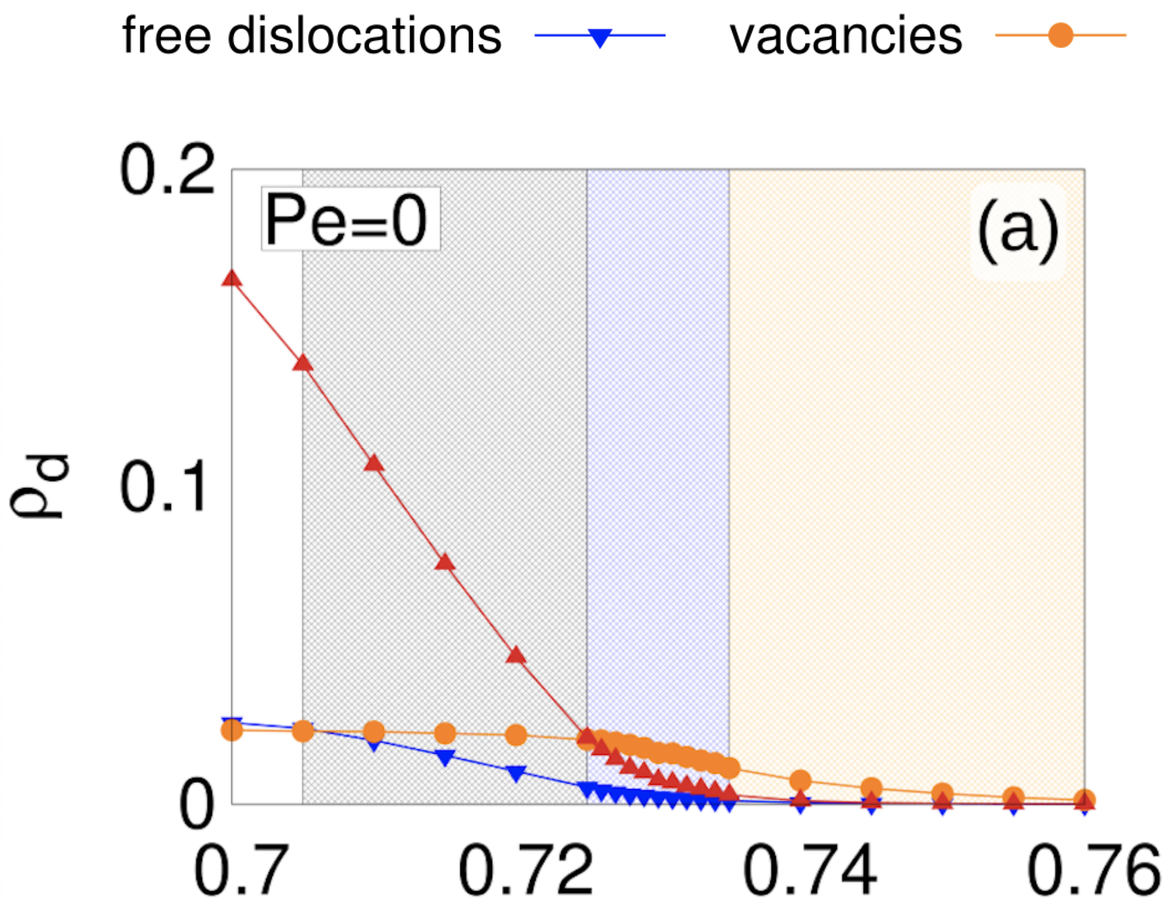

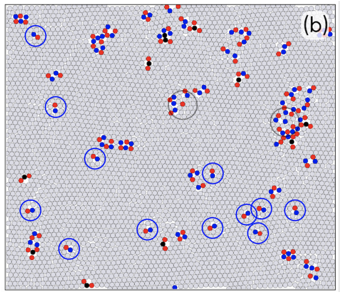

As soon as the liquid appears in co-existence, **defects in clusters dominate**

Clusters of nn defected particles

Percolation : the critical curve

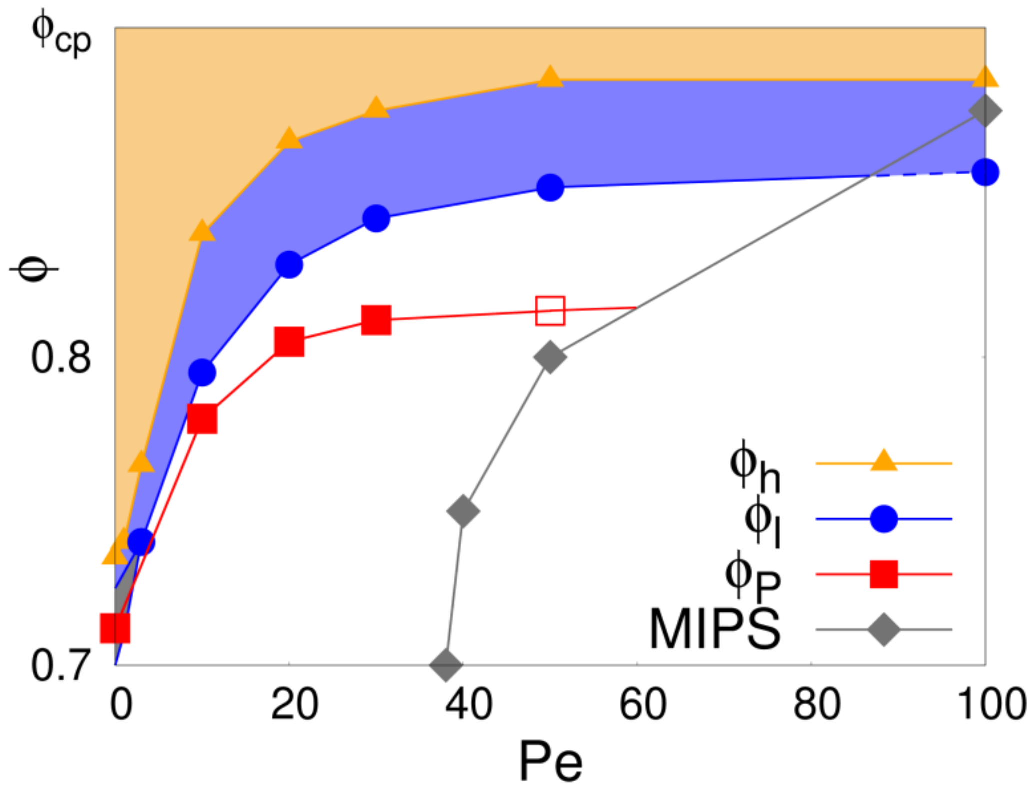

Critical percolation with

fractal properties $d_f \sim 1.9$ and

corresponding algebraic size distribution $\tau \sim 2.05$

Coarse-grained Clusters

Percolation : the critical curve

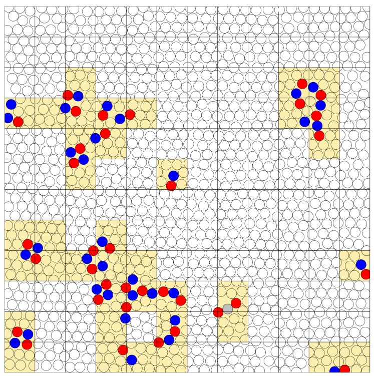

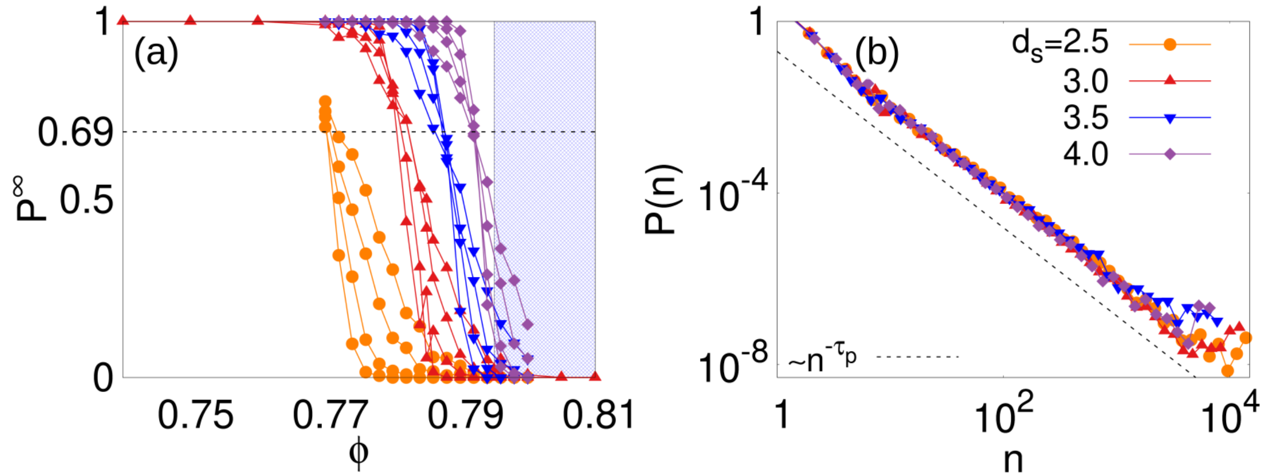

Critical percolation with fractal properties $d_{\rm f} \sim 1.9$ and corresponding algebraic size distribution $\tau \sim 2.05$

With some coarse-graining the **percolation curve** moves upward towards the **hexatic**-**liquid** critical one.

Some open issues

- Is the solid-hexatic transition trully universal ?[1]
  Could ν be constant and not the other exponents ?[2]
- For the liquid-hexatic transition, which are the critical clusters ?
- why is there no difference between the clusters behavior at the first and continuous phase transitions ?

Hard to go further with current numerical methods

[1] **Shi and Chaté, Phys. Rev. Lett. 131, 108301 (2023)** : claims for non-universality of η
[2] **Agrawal, LFC, Faoro, Ioffe & Picco**, in preparation, on a totally different problem !

Active Brownian disks

Questions – à la Statistical Physics

- Pe - ϕ Phase diagram – start from solid and dilute progressively
- Order of, and mechanisms for, the phase transitions.
  - Correlations, fluctuations.
  - Topological defects.
- Motility Induced Phase Separation.
  - Internal structure of dense phase.
  - Mechanisms for growth of dense phase.
- Influence of particle shape, *e.g.* disks *vs.* dumbbells.

Phase Diagram

Solid, hexatic, liquid, co-existence and MIPS

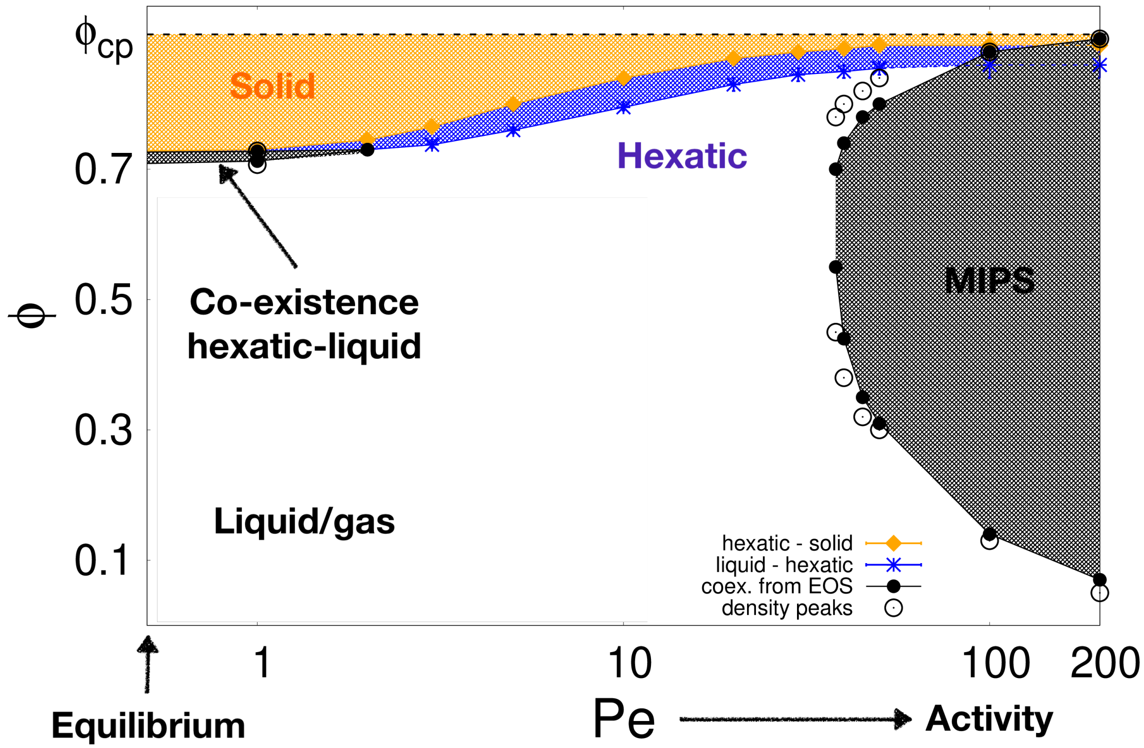

Motility induced

phase separation (MIPS)

gas & dense

Cates & Tailleur

Ann. Rev. CM 6, 219 (2015)

Farage, Krinninger & Brader

PRE 91, 042310 (2015)

Pressure $P(\phi, \text{Pe})$ (EOS), correlations $G_T(r)$, $G_6(r)$, and distributions of ϕ_i, $|\psi_{6i}|$

Digregorio, Levis, Suma, LFC, Gonnella & Pagonabarraga, PRL 121, 098003 (2018)

Motility Induced Phase Separation

The basic mechanism

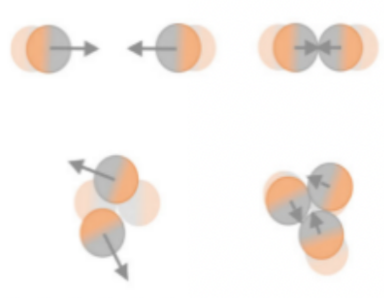

Particles collide heads-on

and cluster even in the

absence of attractive forces

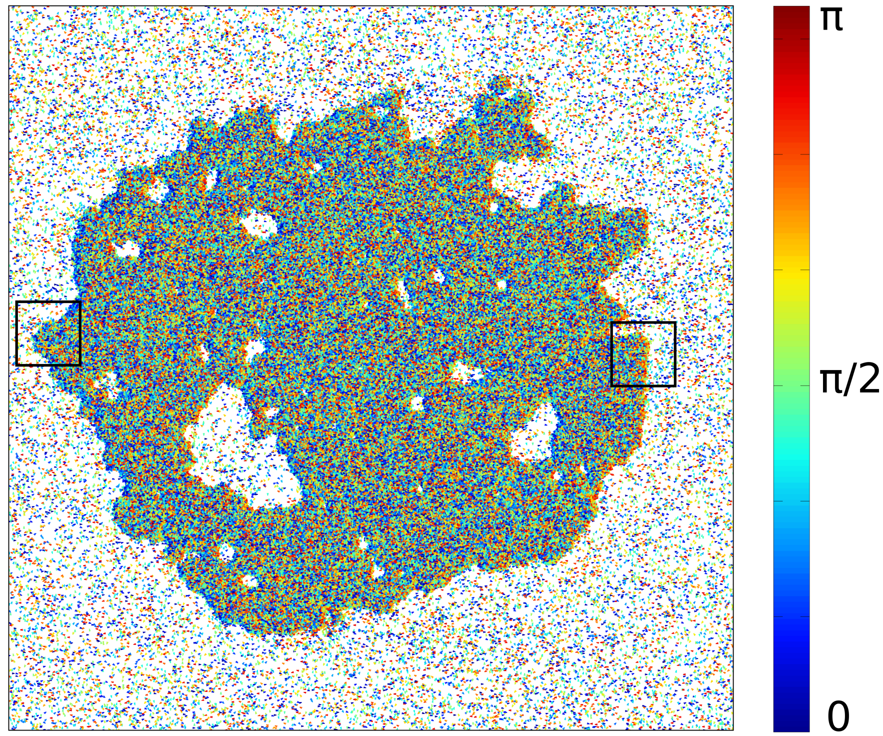

$\longrightarrow$ **blue 0** $\longleftarrow$ **red** π

The colours indicate the direction along which the particles are pushed by the active force $\boldsymbol{F}_{\mathrm{act}}$

MIPS

Local density distributions - dense & gas

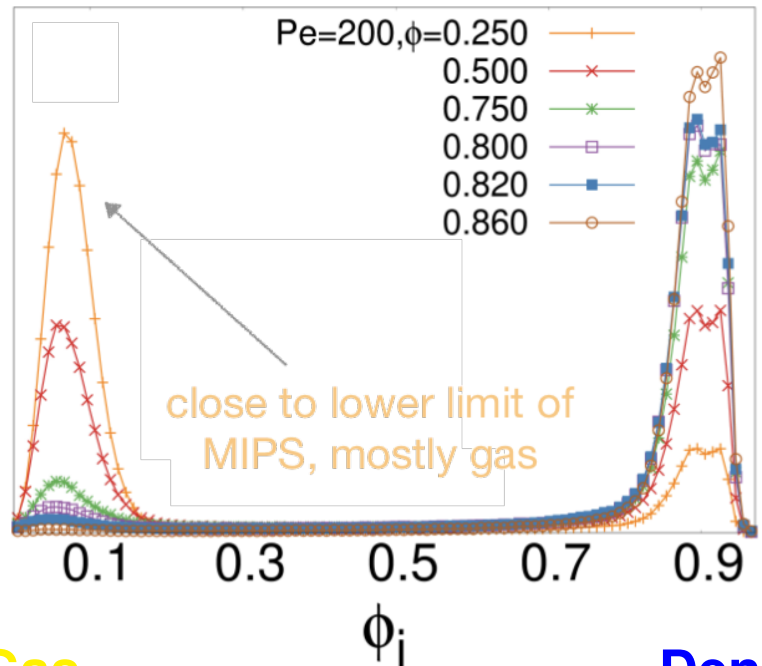

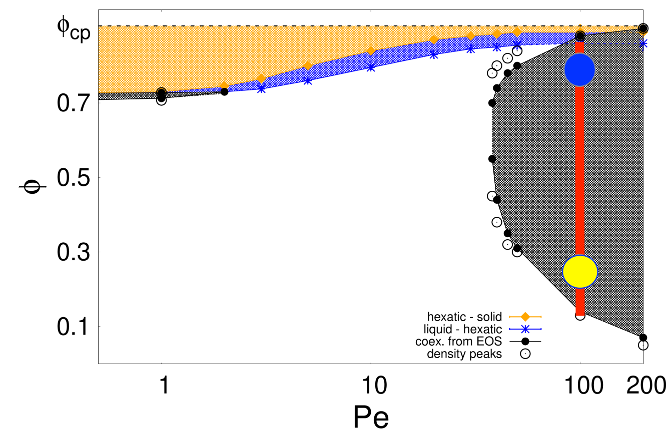

Gas **Dense**

The position of the peaks does not change while changing the global packing fraction ϕ but their relative height does. Transfer of mass from **gas** to **dense** component as ϕ increases

MIPS

Is it just a conventional phase separation ?

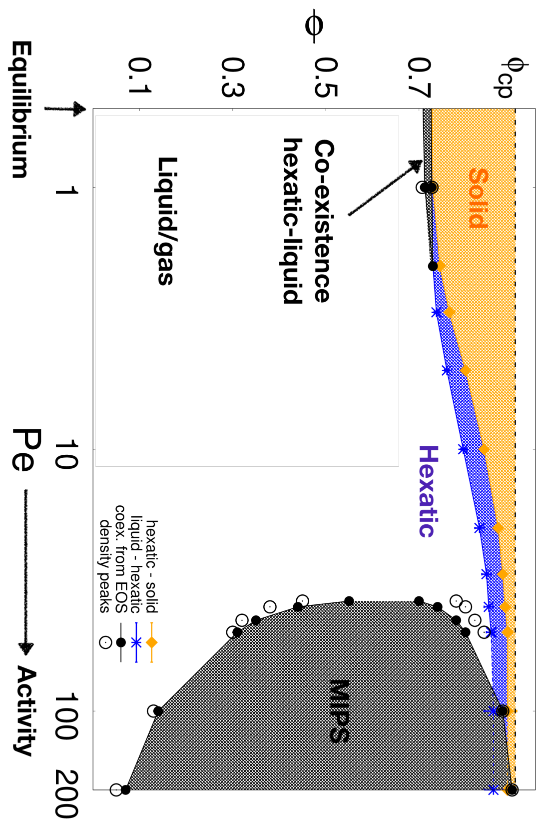

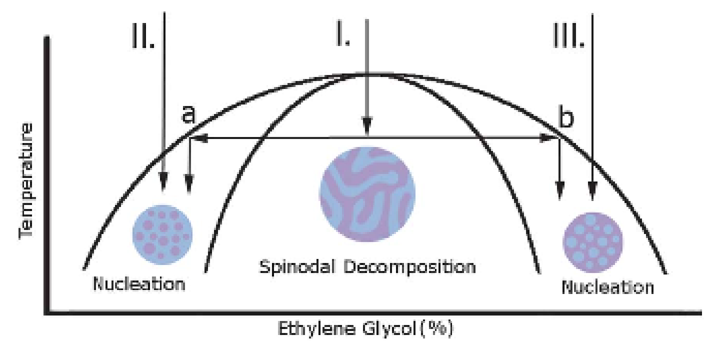

Similar to phase separation with percentage of system covered by dense and gas phases determined by a level rule ?

Cates & Tailleur 12

The dense phase

Hexatic patches, defects, bubbles

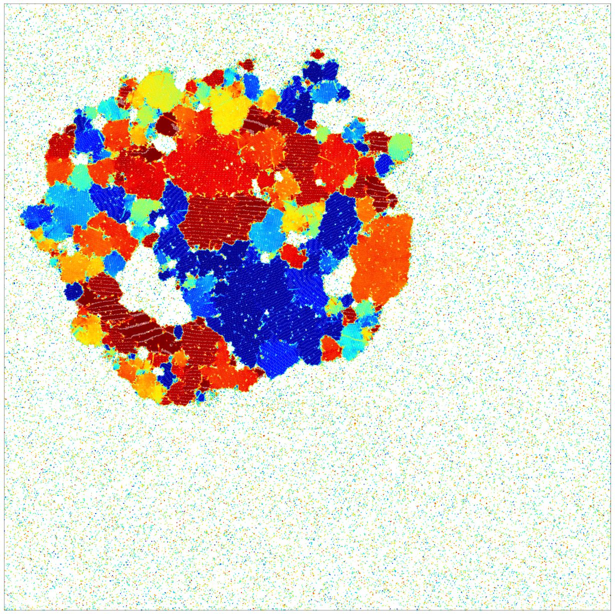

Dense/dilute separation[1]

For low packing fraction ϕ

a single round droplet

Growth[2] of clusters[3] with a mosaic

of hexatic orders[3] with

gas bubbles[2,4,5] & defects[6]

[1] **Cates & Tailleur, Annu. Rev. Cond. Matt. Phys. 6, 219 (2015)**

[2] **Caporusso, Digregorio, Levis, LFC & Gonnella, PRL 125, 178004 (2020)**

[3] **Caporusso, LFC, Digregorio, Gonnella, Levis & Suma, PRL 131, 068201 (2023)**

[4] **Tjhung, Nardini & Cates, PRX 8, 031080 (2018)**

[5] **Shi, Fausti, Chaté, Nardini & Solon, PRL 125, 168001 (2020)**

[6] **Digregorio, Levis, LFC, Gonnella & Pagonabarraga, Soft Matter 18, 566 (2022)**

Structure

Dynamic structure factor $\Rightarrow$ growing length of dense component

I peak:
system average
size

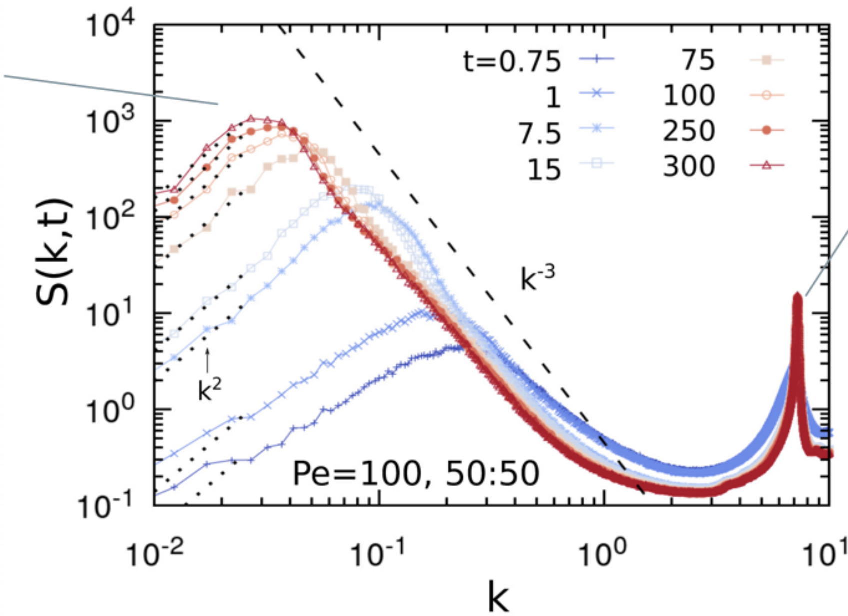

II peak:
particles' packing

$$S(\mathbf{k},t) = \sum_{i=1}^{N} e^{i\mathbf{k}(\mathbf{r_i}-\mathbf{r_j})}$$

related to Fourier transform of the pair correlation function

$$k_{\mathrm{I}}(t) \propto R^{-1}(t)$$

No sign of fractality here. Porod's law $S(k) \sim k^{-(d+1)}$ for compact domains with sharp interfaces

The growth law

Growing length of the dense component and regimes

Different Pe

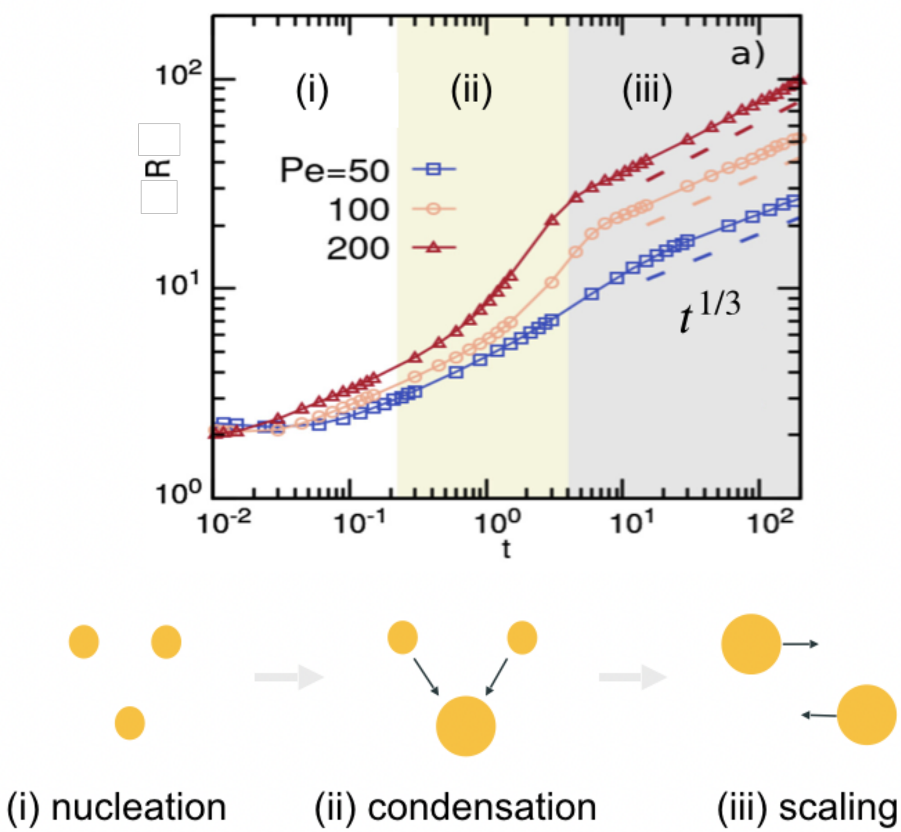

Movie

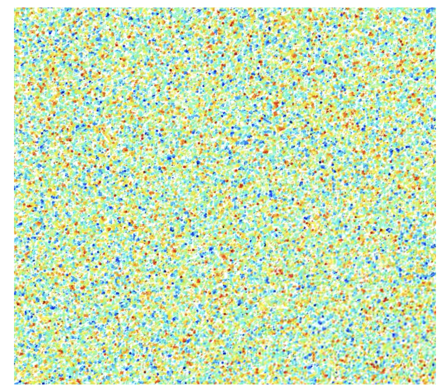

$$R(t) \to aL$$

In scaling regime $t^{1/3}$ like in **Lifshitz-Slyozov-Wagner**, scalar phase separation.

More about it & asymptotic value later

Local hexatic order

Growing length of the orientational order – regimes

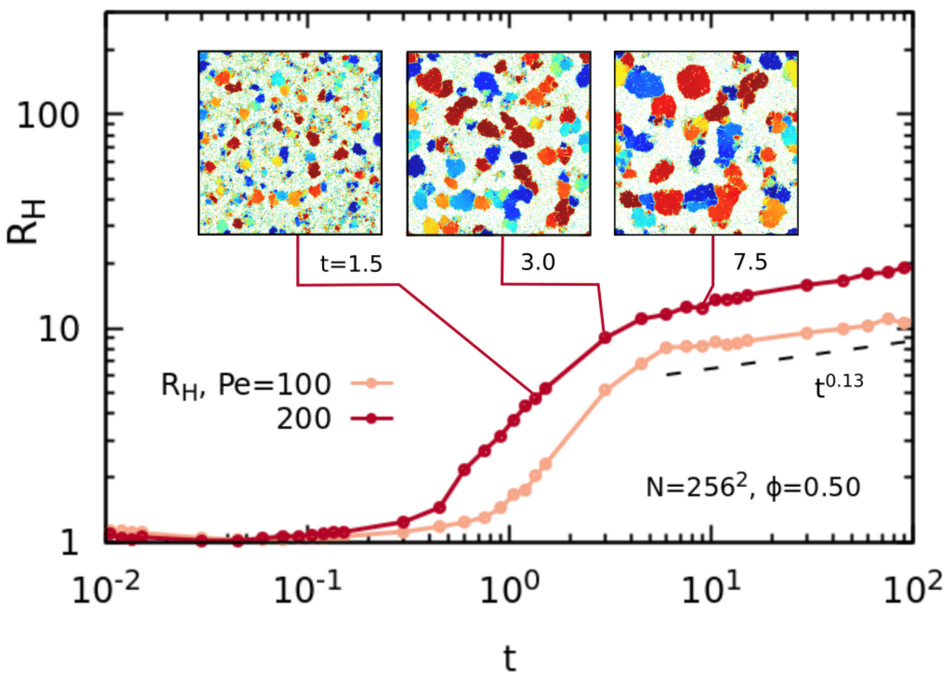

Local hexatic order parameter

$$\psi_{6j} = \frac{1}{nn_j} \sum_{k=1}^{nn_j} e^{i6\theta_{jk}}$$

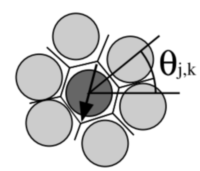

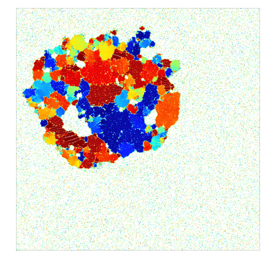

Full hexatically ordered small clusters

Larger clusters with several orientational order within

$R_H \sim t^{0.13}$ in the scaling regime and $R_H \to R_H^s \ll L$

Similar to pattern formation, e.g.

Vega, Harrison, Angelescu, Trawick, Huse, Chaikin & Register, PRE 71, 061803 (2005)

Bubbles in cavitation

At the internal interfaces bubbles pop up

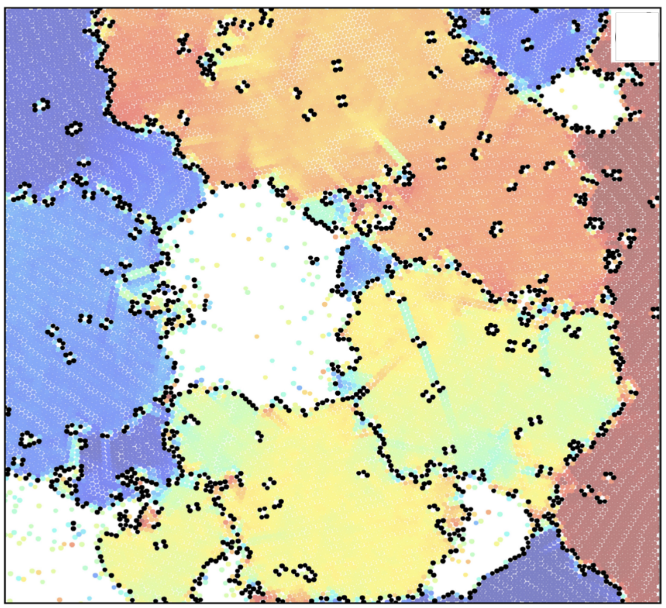

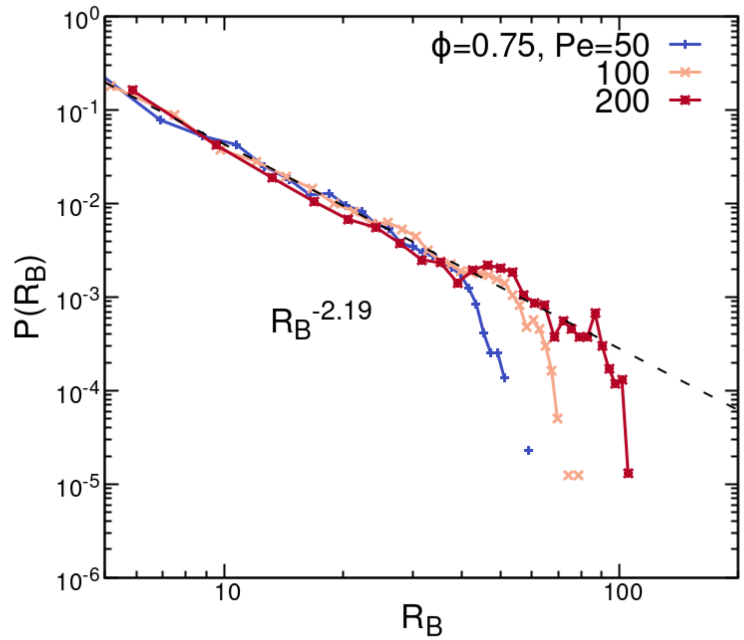

Bubbles appear and disappear at the interfaces between hexatic patches

Algebraic distribution of bubble sizes with a Pe-dependent exponential cut-off

Growth of the dense phase

Beyond what has been done: focus on the clusters

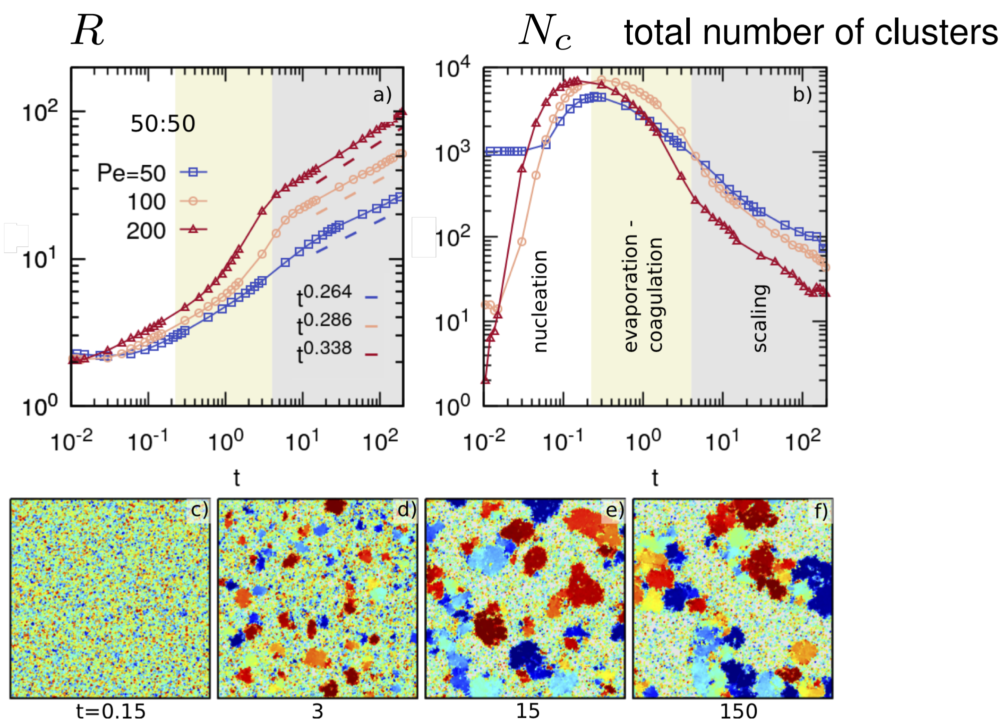

Nucleation Evap/coag Scaling

On the averaged scaling regime and the $t^{1/3}$:

Redner, Hagan & Baskaran, PRL 110, 055701 (2013)

Stenhammar, Marenduzzo, Allen & Cates, Soft Matter 10, 1489 (2014)

Caporusso, Digregorio, Levis, LFC & Gonnella, PRL 125, 178004 (2020)

Beyond?

Goal, answer the questions :

1. Is the growth like the one of **passive attractive particles** ?

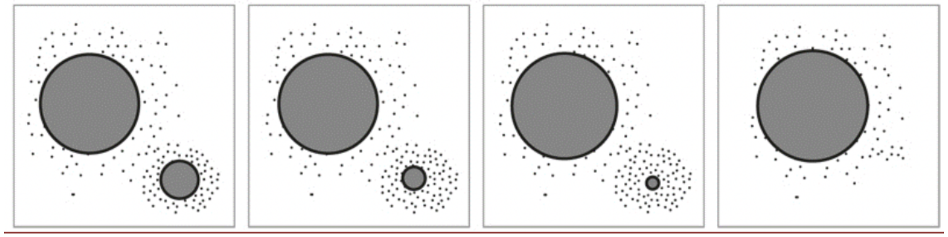

Ostwald ripening

2. Are there other **mechanisms** at work in the active case ?

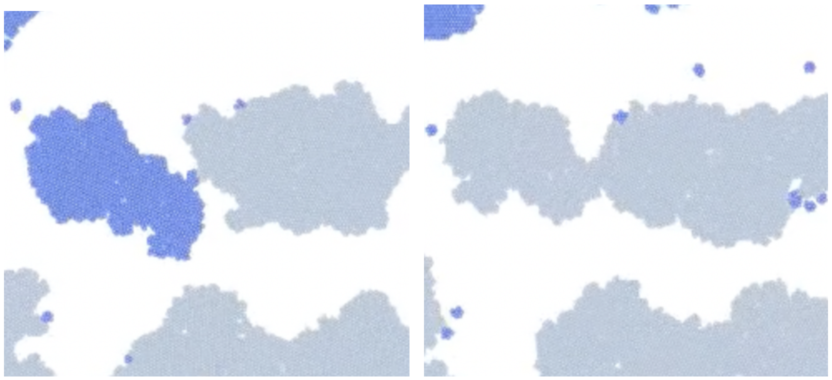

Cluster-cluster aggregation

Dense clusters

Instantaneous configurations (DBSCAN)

Passive - attractive

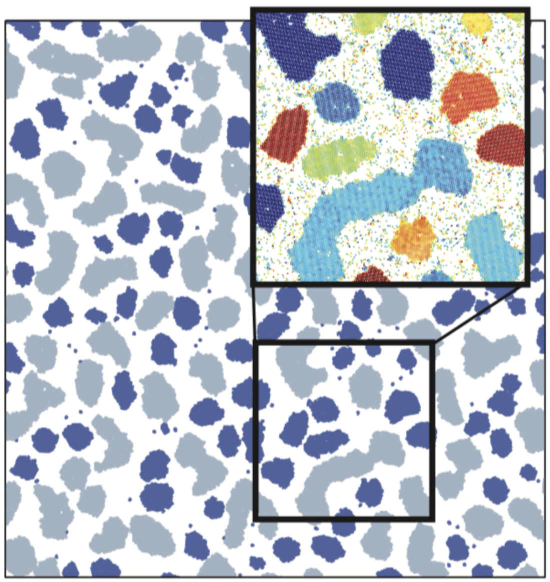

Active - repulsive

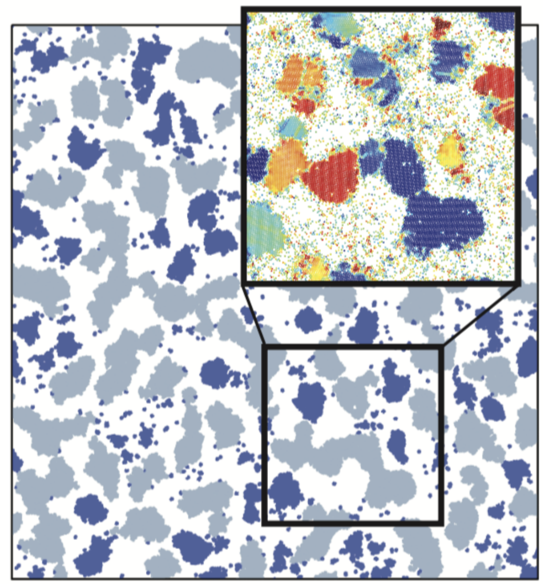

The Mie potential is not truncated in the passive case $\Rightarrow$ attractive

Parameters are such that $R(t)$ is the same in the two systems

Colors in the zoomed box indicate orientational order

Caporusso, LFC, Digregorio, Gonnella, Levis & Suma, PRL 131, 068201 (2023)

Dense clusters

Visual facts about the instantaneous configurations

Similarities

- Large variety of shapes and sizes (masses)

  Co-existence of

  small regular (**dark blue**) and large elongated (**gray**) clusters

Differences

- Rougher interfaces in active
- Homogeneous (passive) vs. heterogeneous (active) orientational order within the clusters

Cluster dynamics

Tracking of individual cluster motion - video

Active

Passive

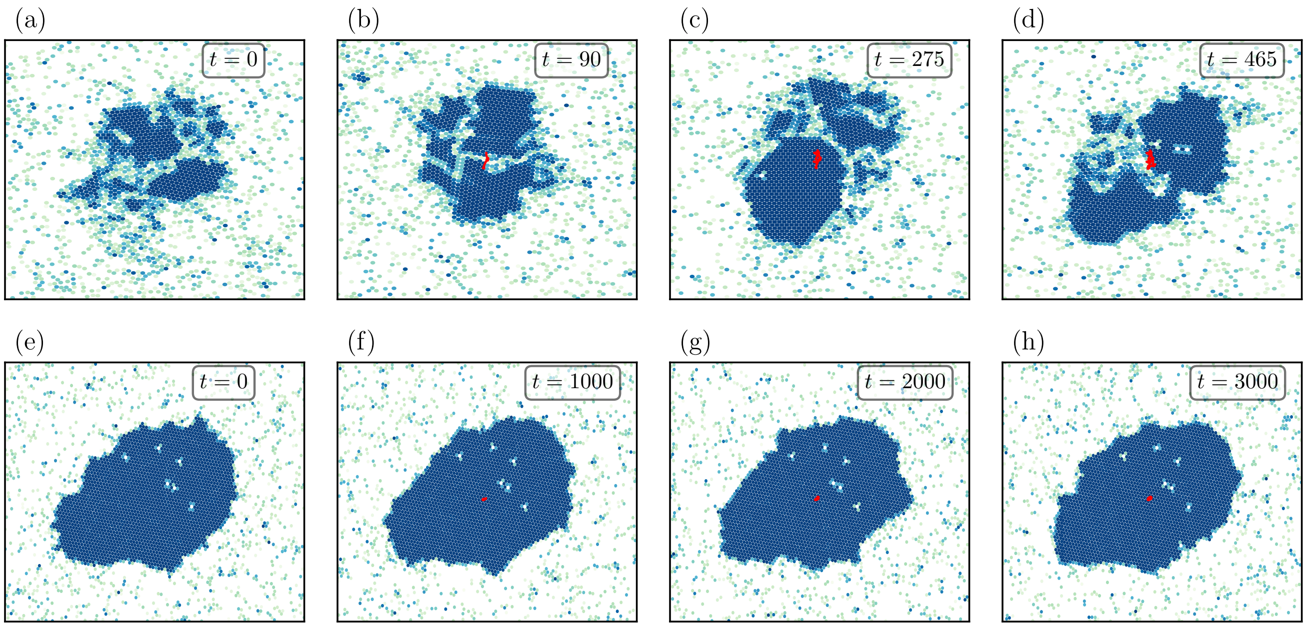

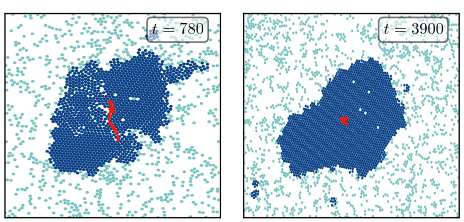

In **red** the center of mass trajectory

Active is much faster than passive

Dense clusters

Visual facts about the cluster dynamics

In both cases, **Ostwald ripening** features

- small clusters evaporate
- gas particles attach to large clusters

In the **active system**

- clusters displace much more & sometimes aggregate
- they also break & recombine

like in **diffusion limited cluster-cluster aggregation**

Dense clusters

Averaged mass

$$\overline{M} \equiv \frac{1}{N_c(t)} \sum_{\alpha=1}^{N_c(t)} M_\alpha(t) \sim t^{2/3}$$

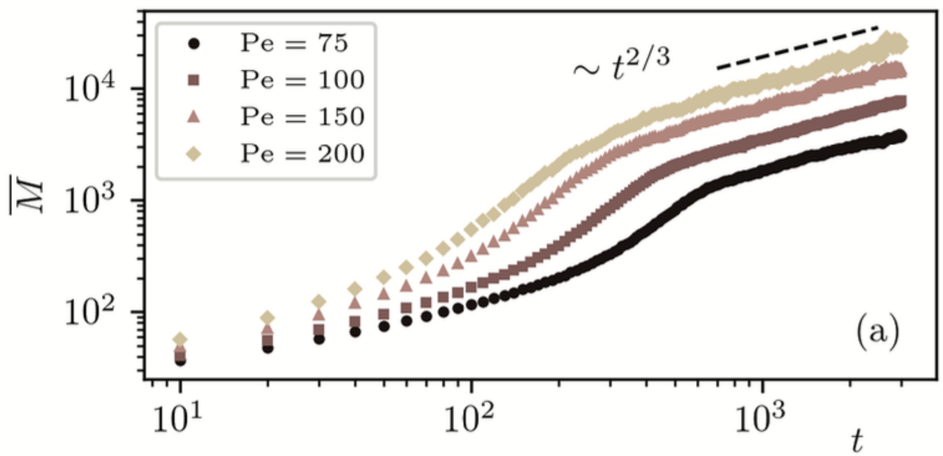

Same three regimes as in R from the structure factor

Clusters' dynamics origin ?

Dense clusters

Mean Square Displacement: diffusion

Average over all clusters

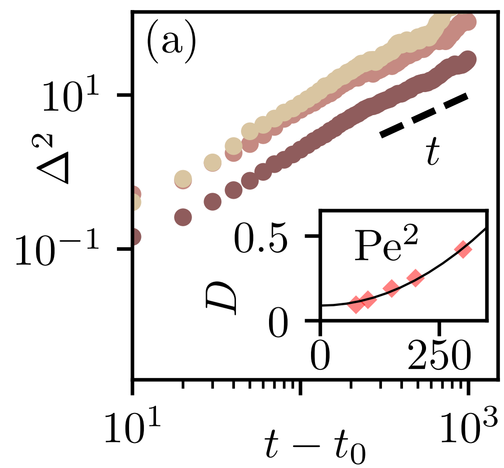

Mass dependence

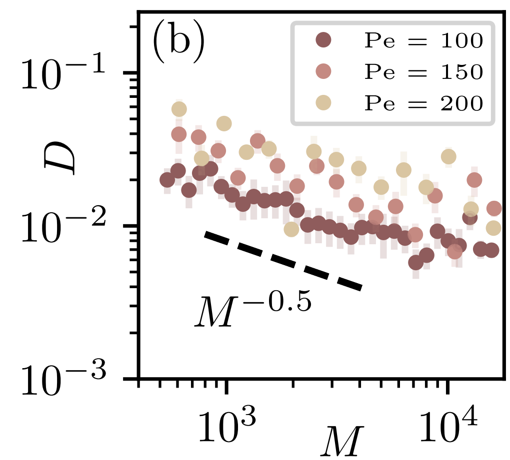

$$\Delta_k^2(t,t_0) = [\mathbf{r}^{(k)}_{\mathrm{c.o.m.}}(t) - \mathbf{r}^{(k)}_{\mathrm{c.o.m.}}(t_0)]^2 \sim 2d\, D(M_k, \mathrm{Pe})\,(t-t_0)$$

A sum of random forces yields $D \sim M^{-1}$

Passive tracer in a dilute active bath $D \sim R^{-1} \sim M^{-1/2}$ **Solon & Horowitz (22)**

Passive & very heavy isolated active clusters $D \sim M^{-1}$

Geometry

Scatter plots : small regular – large fractal

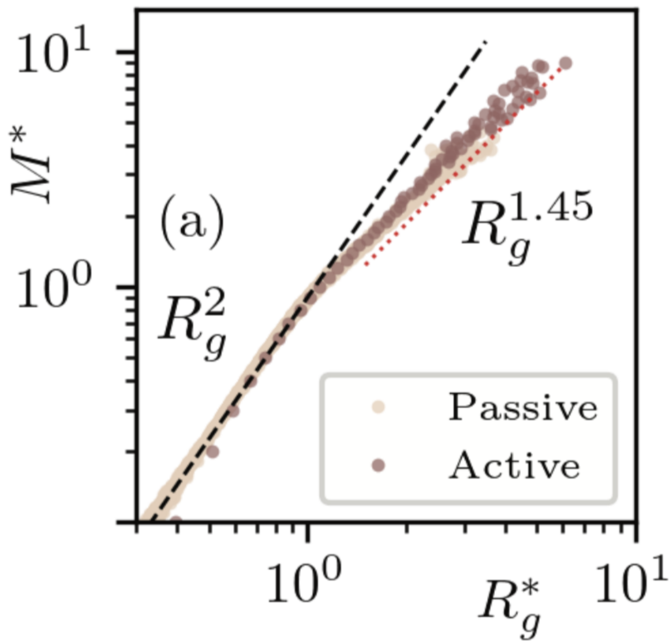

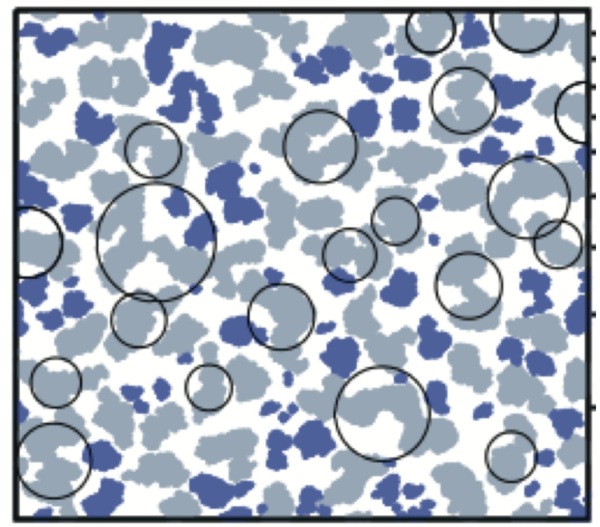

Cluster mass $M^*(t) = \dfrac{M_k(t)}{\overline{M}(t)}$ Gyration radius $R_g^*(t) = \dfrac{R_{g\,k}(t)}{\overline{R_g}(t)}$

Data sampled in the scaling regime $t = 10^3 - 10^5$ every 10^3 time steps

$\overline{M}(t) = \dfrac{1}{N_c(t)} \sum_{k=1}^{N_c(t)} M_k(t)$ and $N_c(t)$ the total number of clusters at time t

Cluster-cluster aggregation

Extended Smoluchowski argument

From $\overline{R}_g \sim t^{1/z}$ and using $D(M) \sim M^{-\alpha}$

Smoluchowski eq. $\Rightarrow z = d_f(1+\alpha) - (d - d_w)$

Regular clusters $M < \overline{M}$

$d_f = d = d_w = 2$

$\alpha = 0.5$

$z = 2(1+0.5) = 3$

Fractal clusters $M > \overline{M}$

$d_f = 1.45, d = 2$ and $d_w \sim 2$

$\alpha = 0.5$ in the bulk

$z = 1.45(1+0.5) = 2.18 < 3$

Reviews on the application of fractals to colloidal aggregation

R. Jullien, Croatia Chemica Acta 65, 215 (1992) P. Meakin, Physica Scripta 46, 295 (1992)

Regular vs fractal clusters

Radius of gyration and number

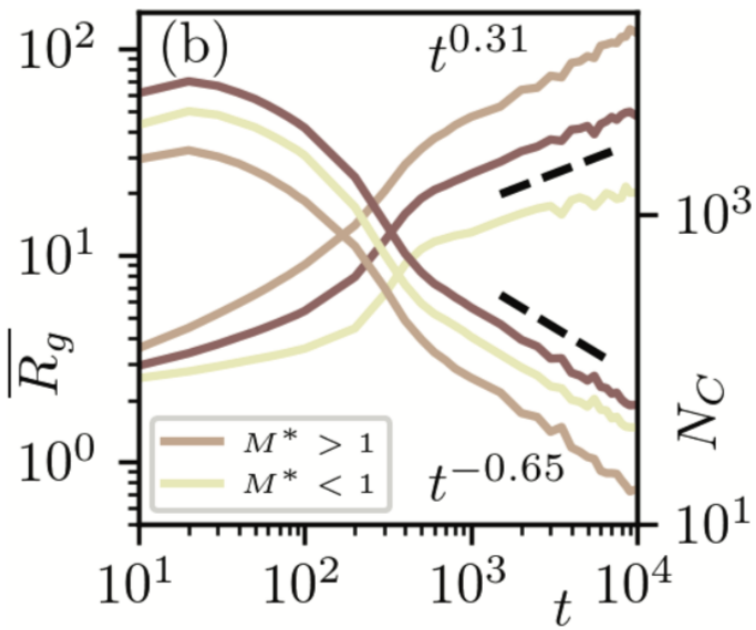

regular $z \gtrsim 3$ | fractal $z < 3$ | average $z = {}^{1}/_{0.31} \sim 3$

More | Less | All

Dominate

Results I on ABPs

We established the full

phase diagram of ABPs

solid, **hexatic**, **liquid** & **MIPS**

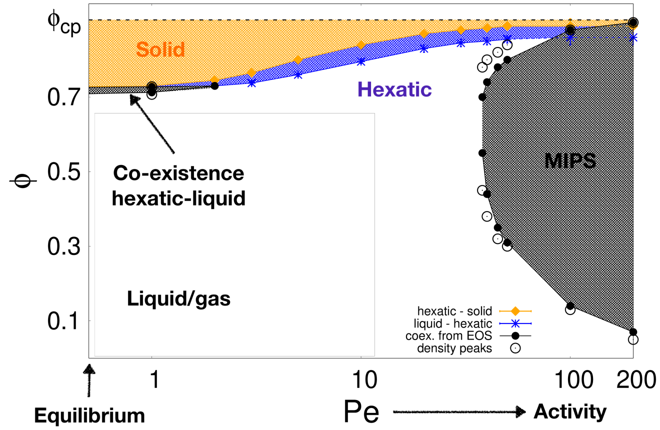

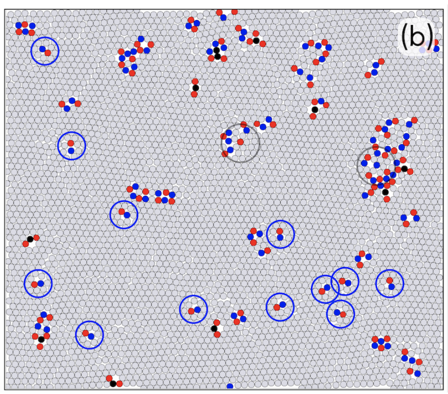

We clarified the role played by point-like

(**dislocations** & **disclinations**)

and **clustered** defects in

passive & active $2d$ models.

In **MIPS**

Micro *vs.* macro: hexatic patches & bubbles

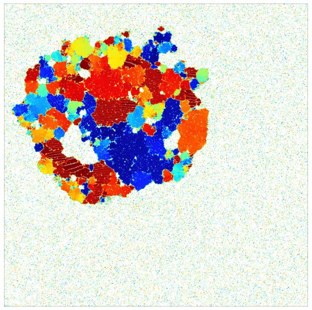

Results II on ABPs

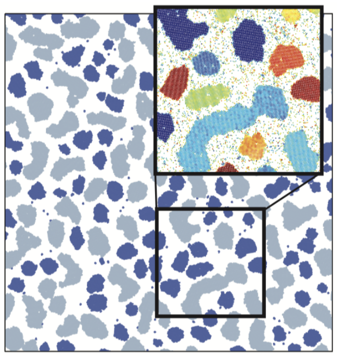

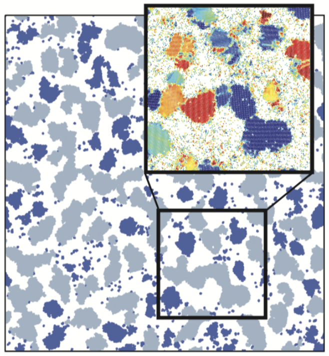

Difference between

Passive

Active

growth

Ostwald ripening & cluster-cluster diffusive aggregation in active case
cluster-cluster aggregation almost not present in passive

Co-existence of regular and fractal clusters in both cases

Heterogeneous orientational order in large active clusters only

Active Brownian disks

Questions – à la Statistical Physics

- Pe - ϕ Phase diagram – start from solid and dilute progressively

- Order of, and mechanisms for, the phase transitions.
  - Correlations, fluctuations.
  - Topological defects.

- Motility Induced Phase Separation.
  - Internal structure of dense phase.
  - Mechanisms for growth of dense phase.

- Influence of particle shape, *e.g.* disks *vs.* **dumbbells**.

Active dumbbell

Diatomic molecule - toy model for bacteria

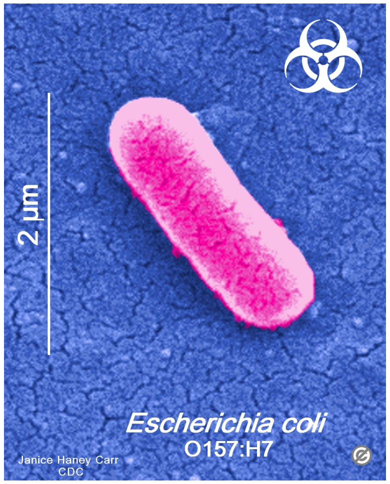

Escherichia coli

Picture borrowed

from the internet

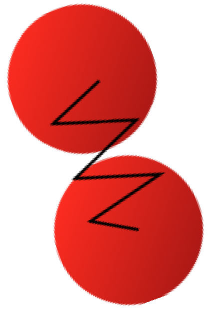

A dumbbell

Active Dumbbells

e.g., a diatomic molecule or a dumbbell

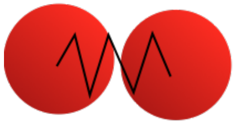

Two spherical atoms with diameter σ_d and mass m_d

Massless spring modelled by a finite extensible non-linear elastic (fene) force between the atoms $\mathbf{F}_\mathrm{fene} = -\dfrac{k(\boldsymbol{r}_i - \boldsymbol{r}_j)}{1 - r_{ij}^2/r_0^2}$ with an additional repulsive contribution (WCA potential) to avoid atomic/colloidal overlapping (see next slides)

Langevin modeling of the interaction with the embedding fluid:

isotropic viscous forces, $-\gamma \boldsymbol{v}_i$, and independent noises, $\boldsymbol{\xi}_i$, on the beads.

Translational motion (centre of mass)

Rotations due to effective torque applied by noise

Vibrations due to the fene potential

Active Dumbbells

a dumbbell made of a colloid 1 and a colloid 2

$$\begin{aligned} m\ddot{\boldsymbol{r}}_1 &= -\gamma\dot{\boldsymbol{r}}_1 + \mathbf{F}_{\mathrm{pot}_1}(\boldsymbol{r}_1,\boldsymbol{r}_2) + \mathbf{F}_{\mathrm{act}} + \boldsymbol{\xi}_1 \\ m\ddot{\boldsymbol{r}}_2 &= -\gamma\dot{\boldsymbol{r}}_2 + \mathbf{F}_{\mathrm{pot}_2}(\boldsymbol{r}_1,\boldsymbol{r}_2) + \mathbf{F}_{\mathrm{act}} + \boldsymbol{\xi}_2 \end{aligned}$$

with $\mathbf{F}_{\mathrm{pot}} = \mathbf{F}_{\mathrm{wca}} + \mathbf{F}_{\mathrm{fene}}$, $V = V_{\mathrm{wca}} + V_{\mathrm{fene}}$ hard and repulsive

$$V_{\mathrm{wca}}(\boldsymbol{r}_1,\boldsymbol{r}_2) = \begin{cases} V_{\mathrm{LJ}}(r_{12}) - V_{LJ}(r_c) & r < r_c \\ 0 & r > r_c \end{cases}$$

$$V_{LJ}(r_{12}) = 4\epsilon\left[\left(\frac{\sigma}{r_{12}}\right)^{2n} - \left(\frac{\sigma}{r_{12}}\right)^{n}\right] \qquad r_c = 2^{1/n}\sigma = \sigma_{\mathrm{d}}$$

Active Dumbbells

a dumbbell made of a colloid 1 and a colloid 2

$$\begin{aligned} m_{\rm d}\ddot{\boldsymbol{r}}_1 &= -\gamma\dot{\boldsymbol{r}}_1 + \mathbf{F}_{{\rm pot}_1}(\boldsymbol{r}_1,\boldsymbol{r}_2) + \mathbf{F}_{\rm act} + \boldsymbol{\xi}_1 \\ m_{\rm d}\ddot{\boldsymbol{r}}_2 &= -\gamma\dot{\boldsymbol{r}}_2 + \mathbf{F}_{{\rm pot}_2}(\boldsymbol{r}_1,\boldsymbol{r}_2) + \mathbf{F}_{\rm act} + \boldsymbol{\xi}_2 \end{aligned}$$

with $\mathbf{F}_{\rm pot} = \mathbf{F}_{\rm wca} + \mathbf{F}_{\rm fene}$, $V = V_{\rm wca} + V_{\rm fene}$ and

$\boldsymbol{\xi}_i$ independent Gaussian thermal noises acting on the two beads,

zero average $\langle \xi^i_a(t)\rangle = 0$ and $\langle \xi^i_a(t)\xi^j_b(t')\rangle = 2\,\gamma k_B T\,\delta_{ij}\delta_{ab}\,\delta(t-t')$.

$i,j = 1,2$ bead labels, $a,b = 1,\dots,d$ coordinate labels

Beyond disks

Phase diagrams & plenty of interesting facts

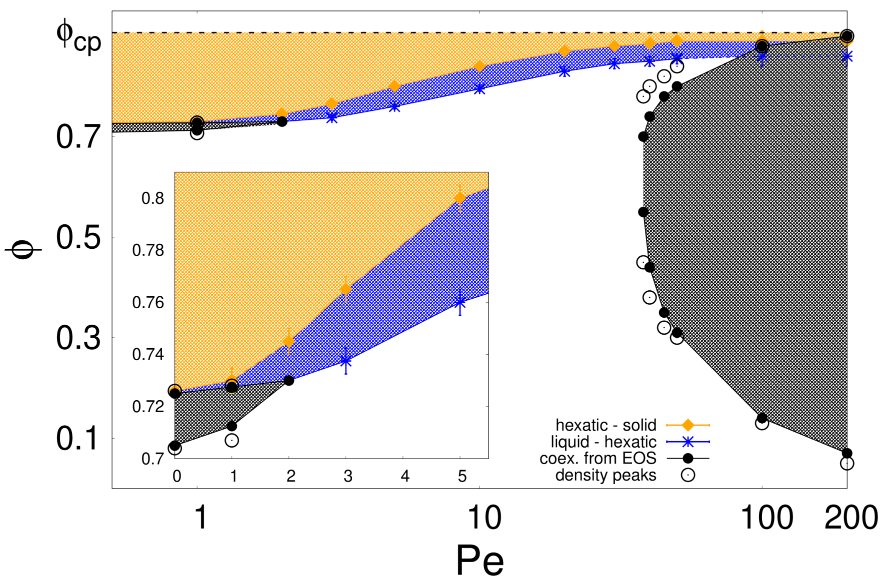

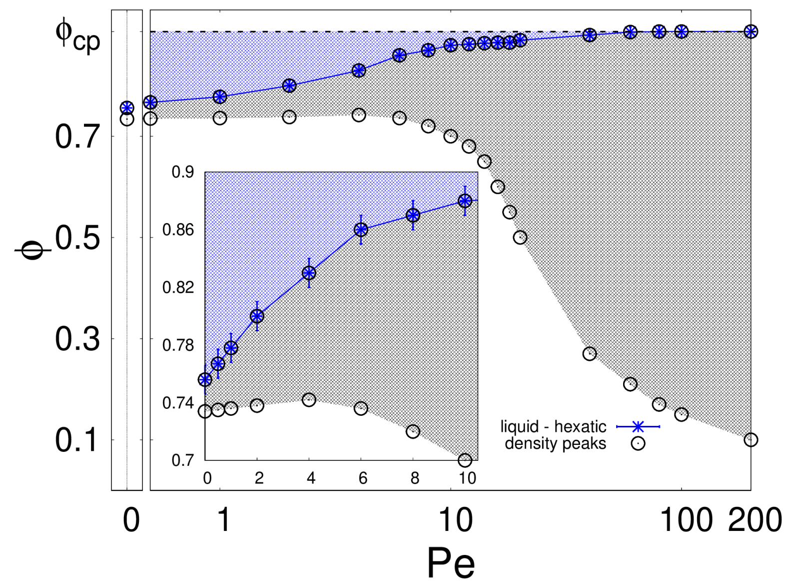

AB Disks **AB Dumbbells**

LFC, Digregorio, Gonnella & Suma, Phys. Rev. Lett. 119, 268002 (2017)

ABPs vs. ABDs

Hexatic order & Correlations

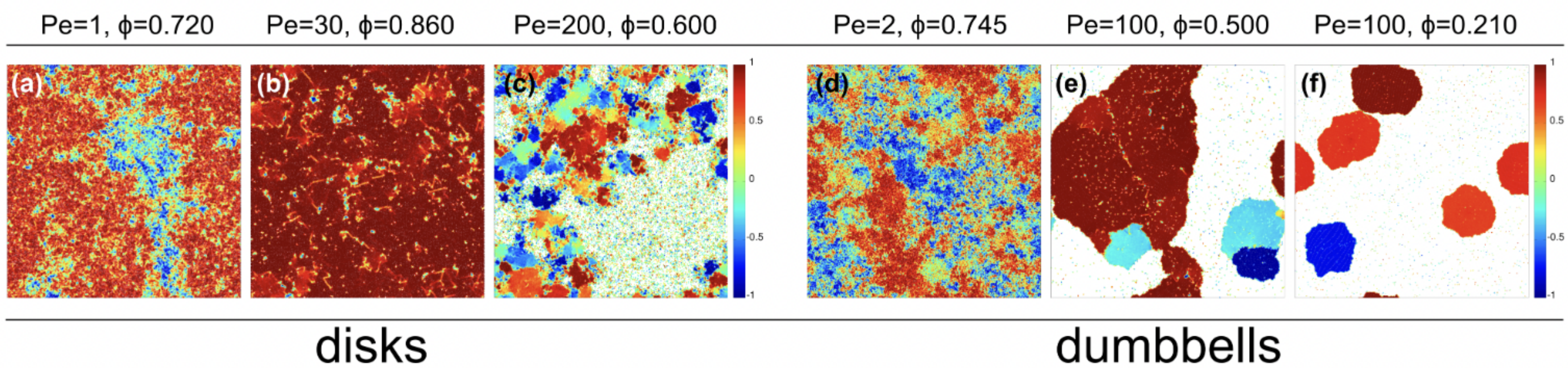

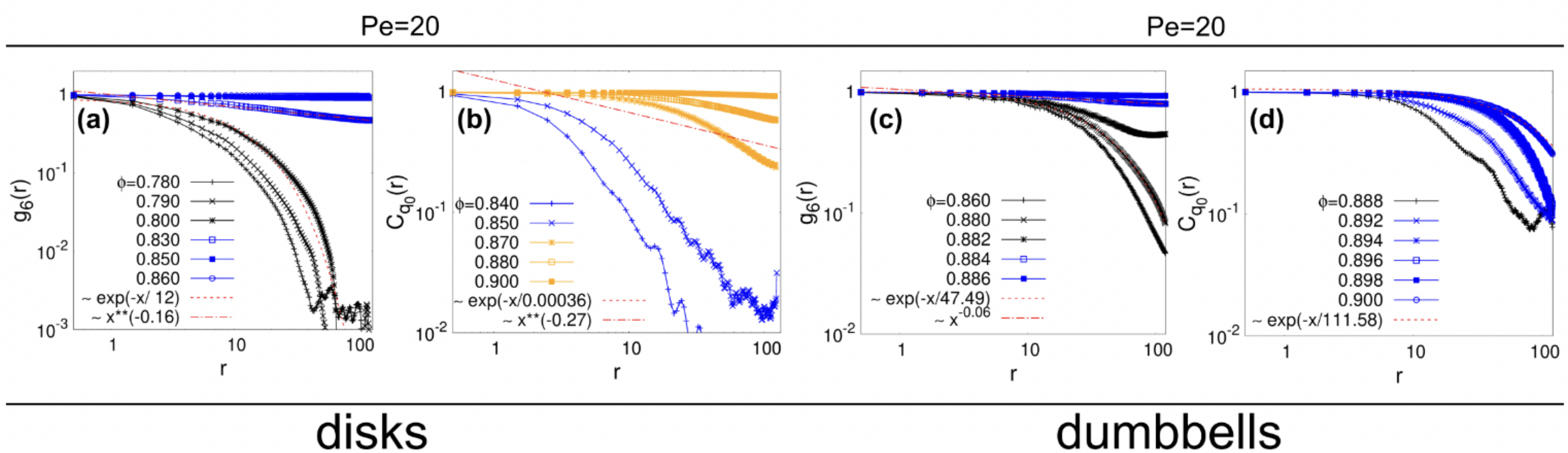

Digregorio, Levis, Suma, LFC, Gonnella, Pagonabarraga, J. Phys. C : Conf. Ser. 1163, 012073 (2019)

ABPs vs. ABDs

Growth of dense phases both at Pe = 100 and 50 :50

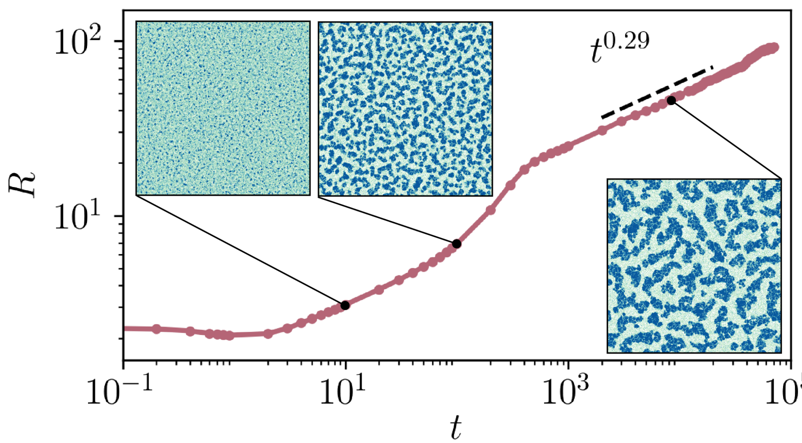

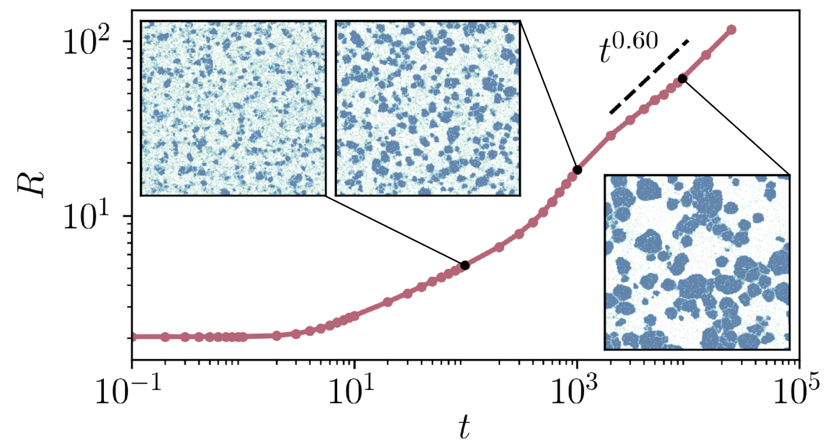

AB Disks

slower

AB Dumbbells

faster

Caporusso, LFC, Digregorio, Gonnella & Suma, Soft Matter (2024)

Active Brownian Dumbbells

Growth of the hexatic order

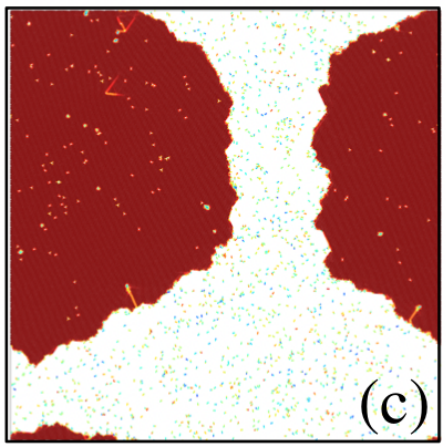

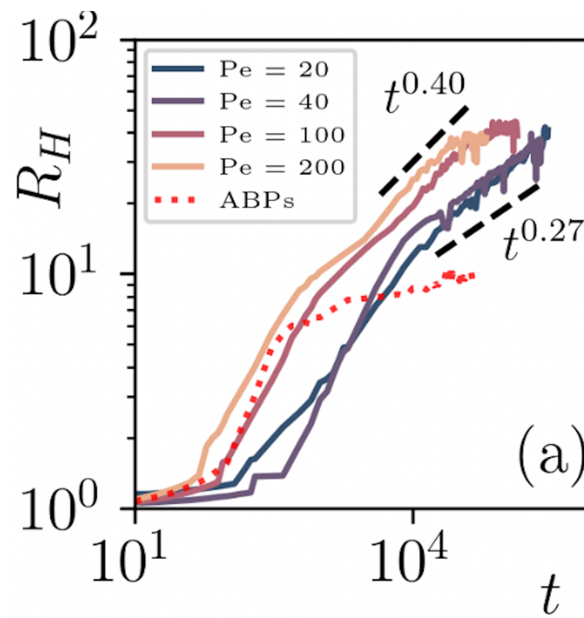

Video

Much faster growth than for ABPs

Full order is reached

No bubbles

Caporusso, LFC, Digregorio, Gonnella & Suma, Soft Matter (2024)

Active Brownian Dumbbells

Motion of isolated dumbbell clusters

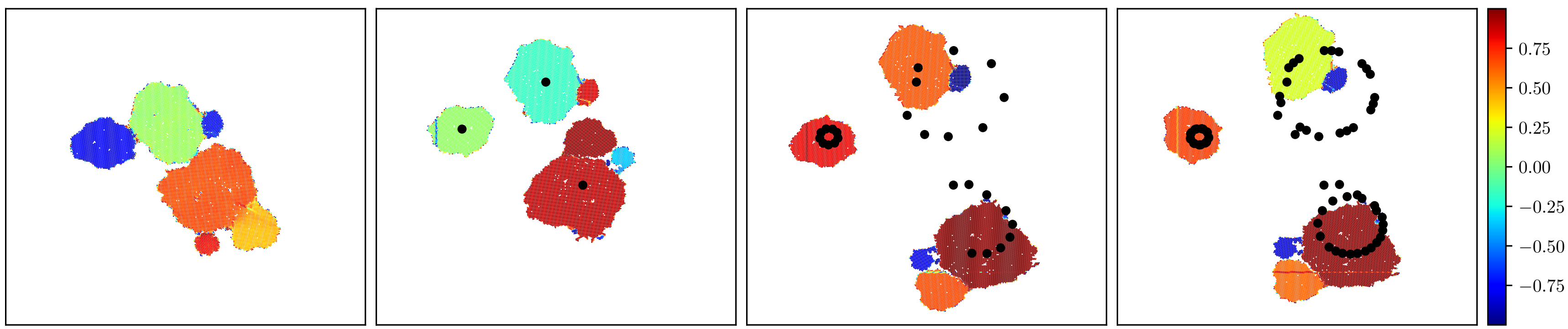

time

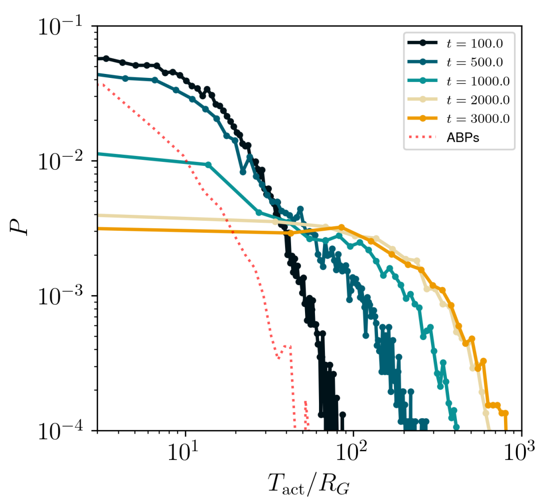

- Instability of clusters with multi-orientational order : they break up along the hexatic interfaces
- The center of mass (c.o.m.) of each cluster α rotates with constant angular velocity ω_α
- The clusters rotate around their c.o.m. with the same angular velocity ω_α

Torque

Solid body motion

Active Brownian Dumbbells

Motion of isolated dumbbell clusters video

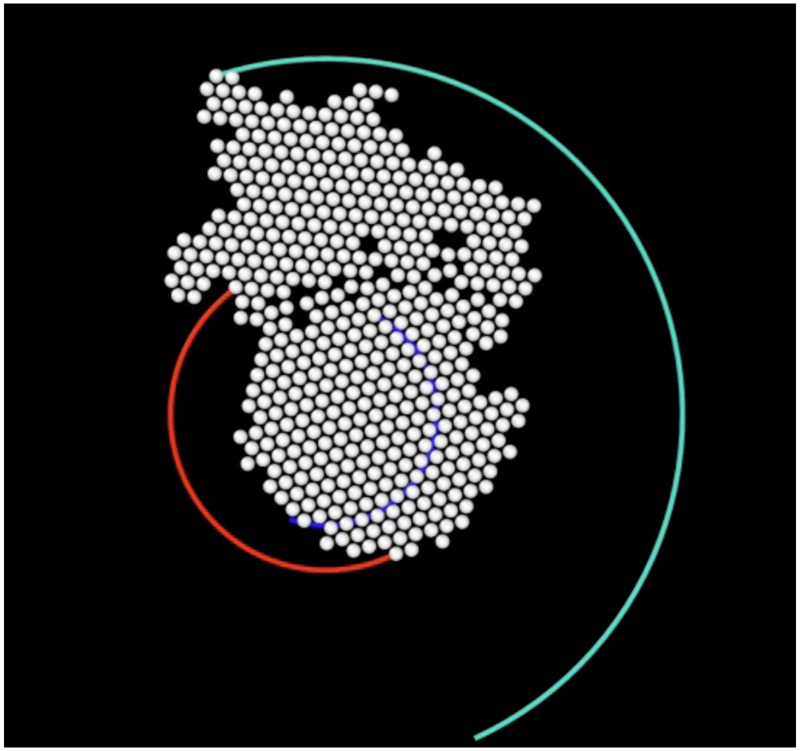

Active Dumbbell clusters

Trajectories

$$\boxed{r = M R_g \frac{F_{\rm act}^{\perp}}{T_{\rm act}}}$$

The radius of the c.o.m. trajectory

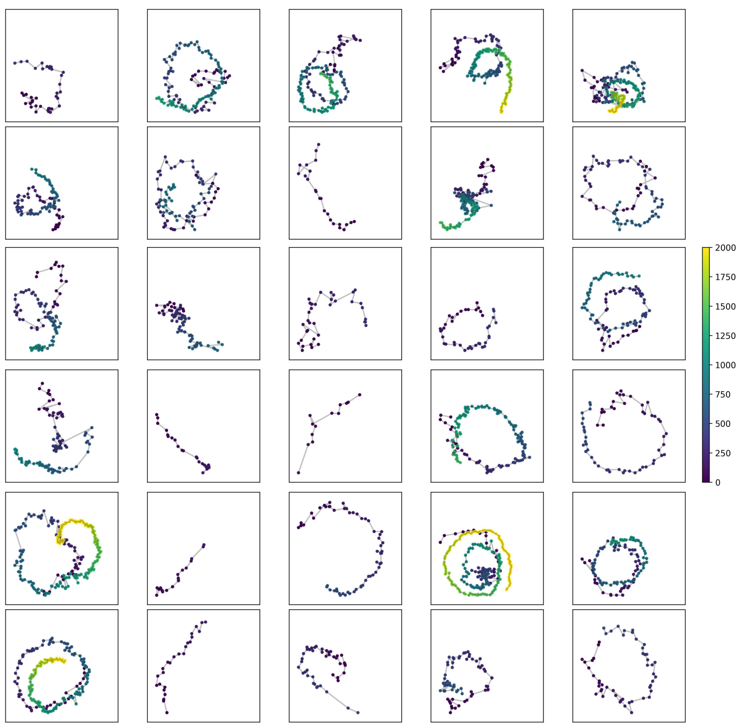

Trajectories in the bulk

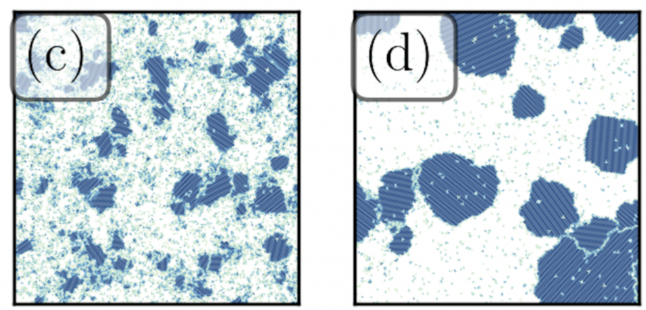

Non-vanishing :

active torque $T_{\rm act}$ & force $F_{\rm act}$

Rotation instead of ABP diffusion

Video

Caporusso, LFC, Digregorio, Gonnella & Suma, Soft Matter (2024)

Results III ABPs vs ABDs

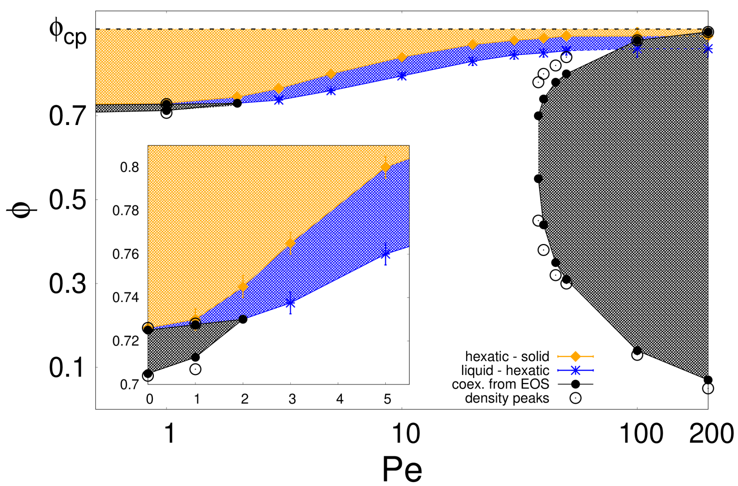

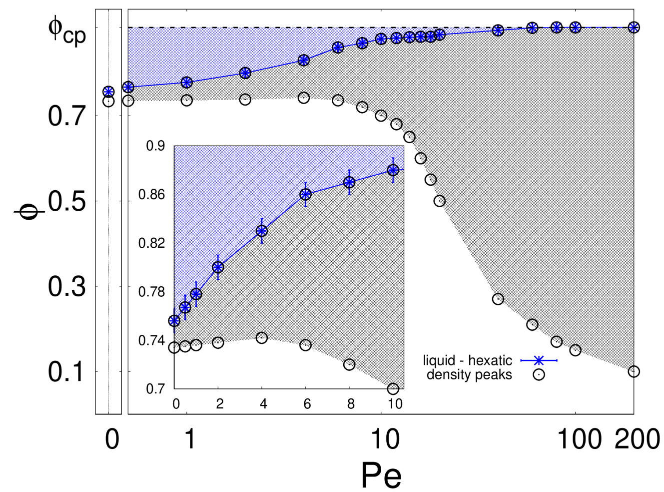

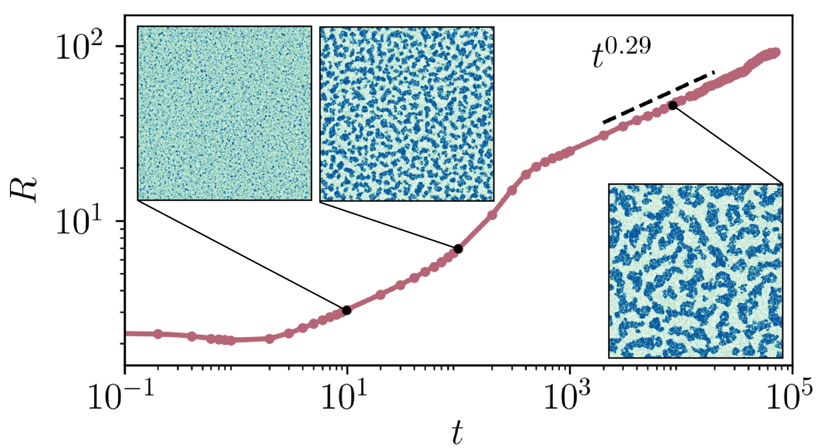

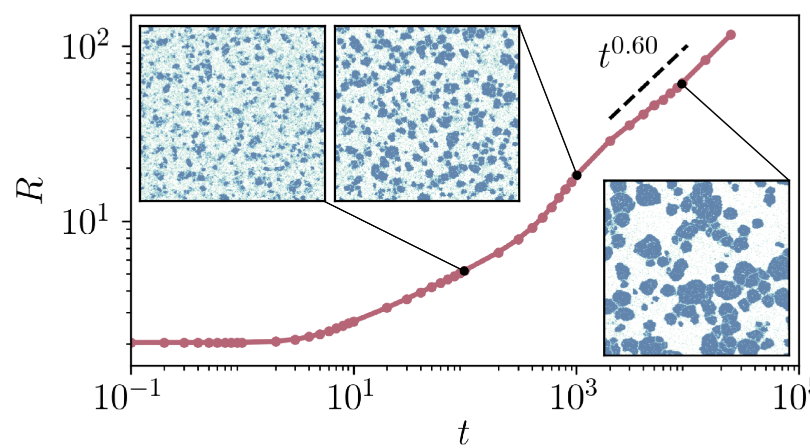

AB Disks

diffusion

AB Dumbbells

rotations

Journal of Statistical Mechanics: Theory and Experiment
an IOP and SISSA journal

Extras

Cluster-cluster aggregation

Extended Smoluchowski argument

From $\overline{R}_g \sim t^{1/z}$ and using $D(M) \sim M^{-\alpha}$

Smoluchowski eq. $\Rightarrow z = d_f(1+\alpha) - (d - d_w)$

Regular clusters $M < \overline{M}$

$d_f = d = d_w = 2$

$\alpha = 0.5$

$z = 2(1+0.5) = 3$

Fractal clusters $M > \overline{M}$

$d_f = 1.45, d = 2$ and $d_w \sim 2$

if, instead, $\boxed{\alpha = 1}$

$z = 1.45(1+1) \sim 3$

Reviews on the application of fractals to colloidal aggregation

R. Jullien, Croatia Chemica Acta 65, 215 (1992) P. Meakin, Physica Scripta 46, 295 (1992)

Dislocations

At the solid-hexatic transition for all Pe $\nu = 0.37$ Universality

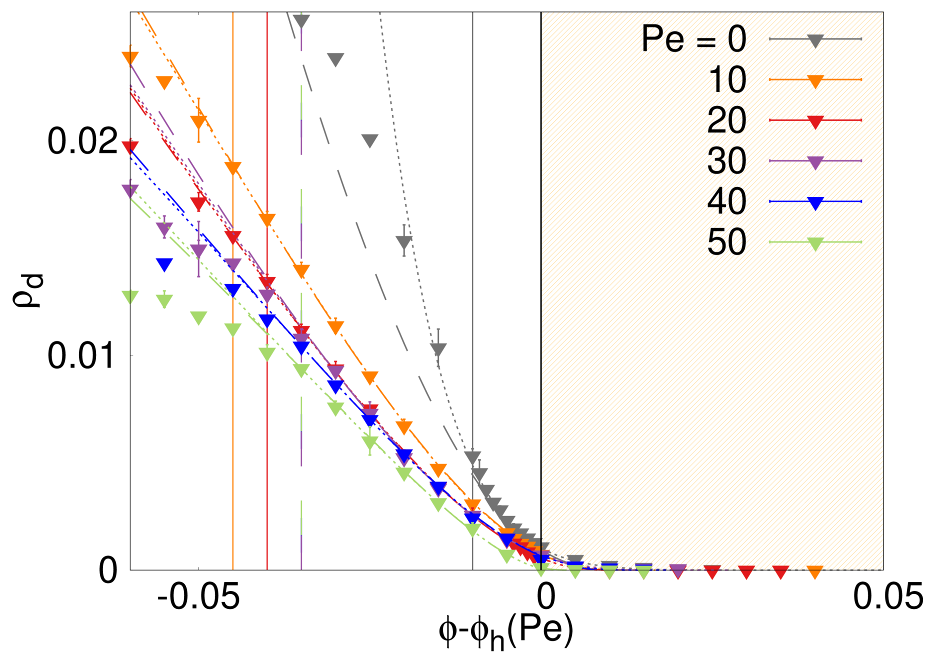

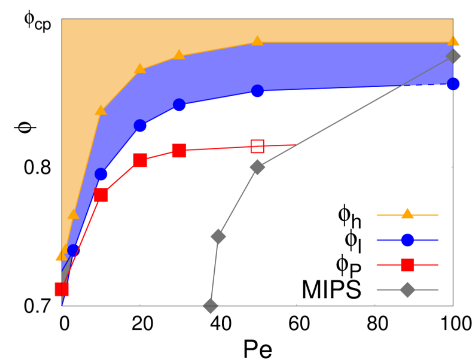

Four (ϕ_c, ν, a, b dotted) vs. three ($\phi_c, \nu = 0.37, a, b$ dashed) parameter fits on data in the hexatic & solid phases only. Criteria to support $\nu = 0.37$:

– χ^2 *cfr.* **Batrouni et al** for $2d$XY

– not crazy values for a, b but crazy values for ν if let to be fitted

– difference between ϕ_c and ϕ_h erased by coarse-graining

Interfaces

Clusters of defects – mostly along hexatic-hexatic interfaces

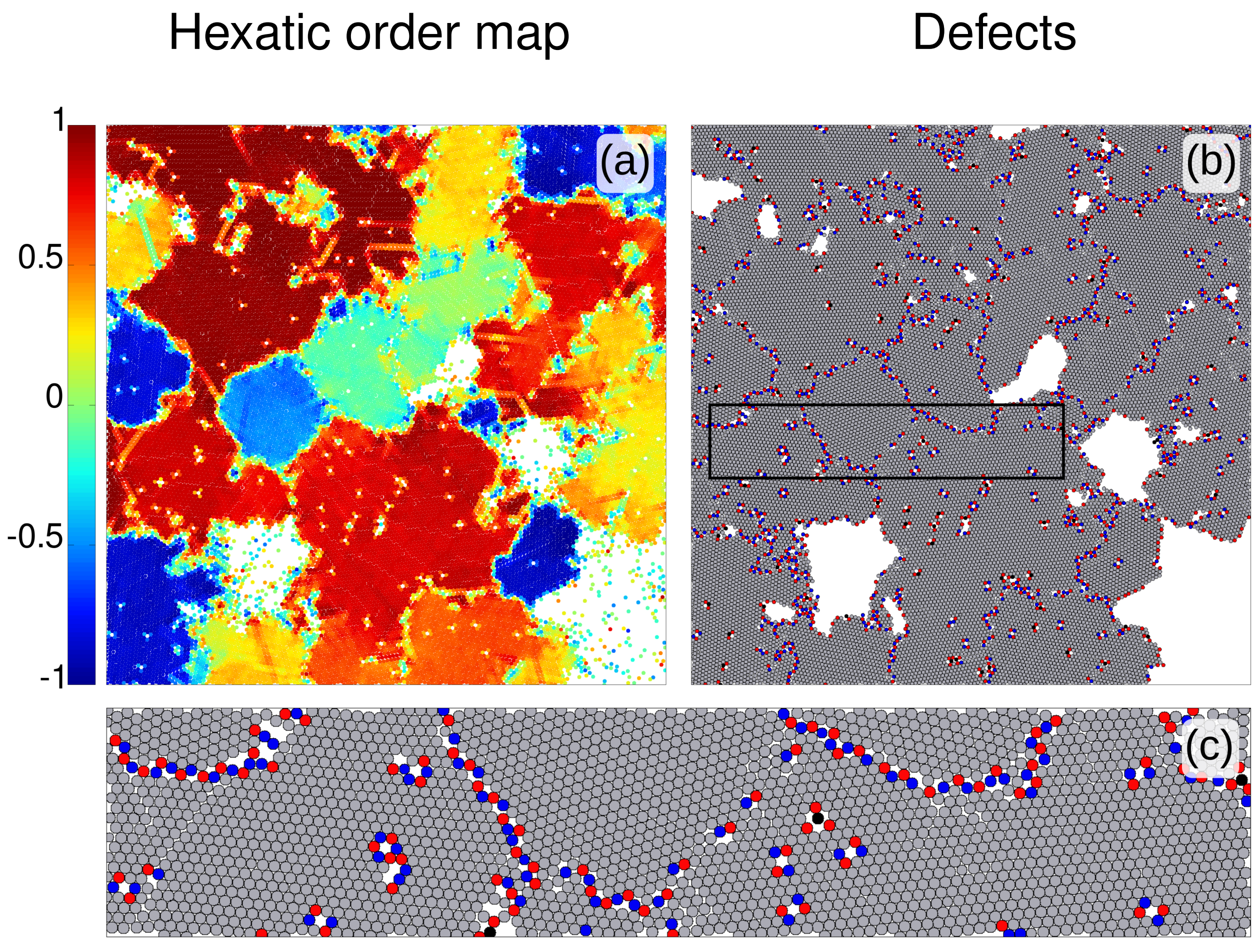

Zoom over the rectangular selection

Clusters of defects

Size distribution - Finite size cut-off

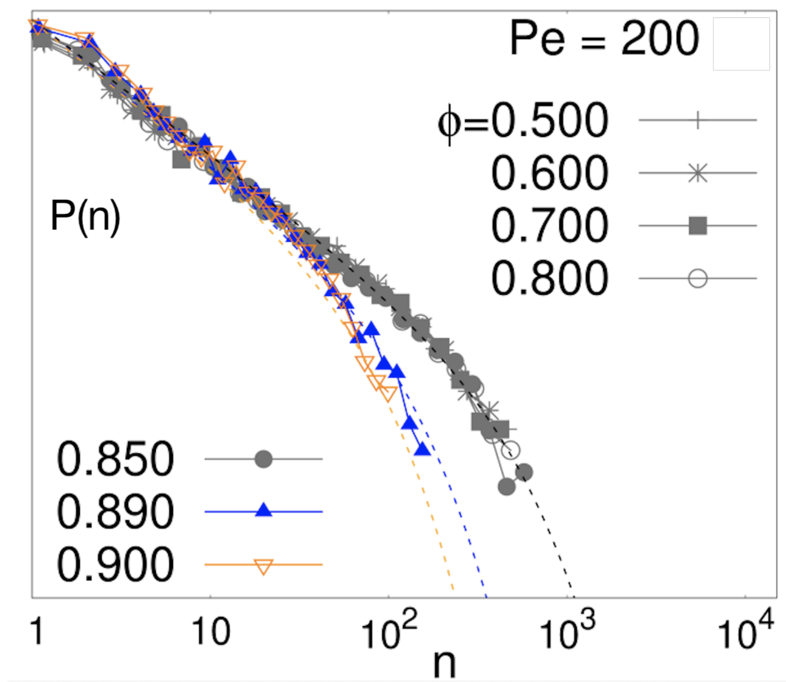

$$P(n) \simeq n^{-\tau} e^{-n/n^*}$$

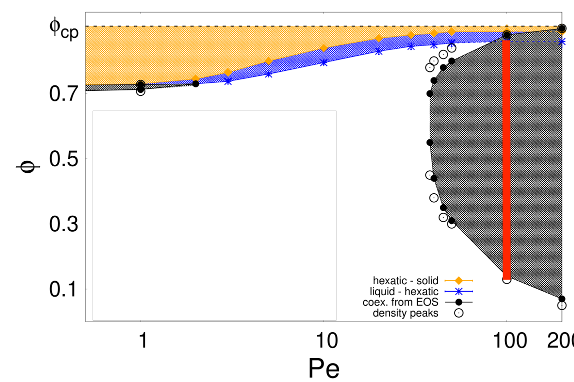

Independence of ϕ at fixed Pe within MIPS

$n^* \sim 30, 50, 200$ in the **solid**, **hexatic** and **MIPS**, respectively, and $\tau \sim 2.2$